SINTEF

TR A7638- Unrestricted

Report

Phase change materials for thermal energy storage in low- and high-temperature applications: a state-of-the-art

SINTEF Energy Research, competence-building project PCM-Eff

Authors
Alexis Sevault, Hanne Kauko, Mette Bugge, Krzysztof Banasiak, Nils Erland Haugen, Øyvind Skreiberg

SINTEF Energy Research
Thermal Energy department
2017-11-30

SINTEF Energi AS
SINTEF Energy Research
Address:
Postboks 4761 Torgarden
NO-7465 Trondheim
NORWAY
Switchboard: +47 73597200

energy.research@sintef.no
www.sintef.no/energi
Enterprise /VAT No:
NO 939 350 675 MVA

KEYWORDS:
Phase change materials, PCM, thermal energy storage, latent heat storage, energy efficiency

Report

Phase change materials for thermal energy storage in low- and high-temperature applications: a state-of-the-art

VERSION
1

DATE
2017-11-30

AUTHOR(S)
Alexis Sevault, Hanne Kauko, Mette Bugge, Krzysztof Banasiak, Nils Erland Haugen, Øyvind Skreiberg

PROJECT NO.
502001554

NUMBER OF PAGES:
53

ABSTRACT
Thermal energy storage (TES) relates to any form of storage of heat or cold, with the aim of utilizing it at a later point of time. Using phase change materials (PCMs) as storage medium, TES is also known as latent heat thermal energy storage (LHTES). PCMs have been studied for more than a decade due their high potential in a wide range of applications. Today, commercial LHTES applications are mainly found for the building sector and for thermal management of power electronics. LHTES applications are expected to reach a wider range of sectors in a near future.

This report presents an overview of PCM properties, the main features of LHTES systems, as well as a number of challenges to overcome with the design of LHTES systems. The focus is on two particular applications: low-temperature LHTES for refrigerated cabinets in food retail stores and high-temperature LHTES for wood stove combustion. The report includes a review on relevant computational fluid dynamics (CFD) modelling techniques and associated challenges.

PREPARED BY
Alexis Sevault

SIGNATURE
A. Sevault

CHECKED BY
Øyvind Skreiberg

SIGNATURE

APPROVED BY
Per N. Mikalsen

SIGNATURE

REPORT NO.
TR A7638

ISBN
978-82-594-3684-9

CLASSIFICATION
Unrestricted

CLASSIFICATION THIS PAGE
Unrestricted

Document history

VERSION	DATE	VERSION DESCRIPTION
0.1	2017-08-25	Final draft sent to review
0.2	2017-09-12	First quality assurance review addressed
0.3	2017-10-17	Second quality assurance review addressed
0.4	2017-11-03	Version submitted to final quality assurance review
1	2017-11-30	Final version

Table of contents

1 Introduction

Thermal energy storage (TES) is needed whenever there is a temporal mismatch between production and demand of thermal energy. TES can be used to store heat or cold during periods of overproduction of heat or electricity, to be able to utilize it at a later point of time. A classical, and the most obvious, example is solar energy applications [1, 2]. However, TES may be applied to reduce peak heating and cooling demands and improve system efficiency wherever there is a variation in the availability and/or demand, on a shorter or longer time scale; and on hourly, diurnal or seasonal basis.

Thermal energy can be stored either in the form of sensible heat, latent heat, or as thermochemical energy [3]. In a sensible heat storage, heat is stored by heating a medium with high specific heat capacity. In a thermochemical heat storage, heat is stored using reversible chemical reactions that absorb or release thermal energy. In the case of latent heat storage, heat is stored as the latent heat of phase change: melting or vaporization. Examples of thermal energy storage methods relying on these three heat processes are given in Table B.1 (Appendix B), as well as key figures illustrating their performance and cost.

Latent heat is unique in that the temperature of the material does not change during the phase change process. A great advantage of latent heat storage is its high energy density as compared to sensible heat storage, resulting in smaller storage volumes. For a given temperature range, their high latent heat of fusion enables PCMs to store 5–14 times more heat per unit volume than common sensible storage materials such as water, masonry, or rock [4]. Furthermore, latent heat storage systems generally are easier to work with than thermochemical storage systems, regarding stability, corrosion and degree of degradation cycle after cycle.

Practical phase change materials (PCMs) are materials that undergo solid-liquid transformation, i.e. a melting-solidification cycle, at around the operating temperature range of the selected thermal application [3]. The heat that is absorbed/released during the melting/solidification process is known as the latent heat of fusion, usually given in $kJ \cdot kg^{-1}$. Figure 1 shows a generic heating curve for a material with phase changes: heating of solid up to the melting point (T_m), followed by melting, heating of liquid up to the evaporation point (T_e), vaporization and finally heating of gas. The figure illustrates that the energy needed to vaporize a material, i.e., the latent heat of vaporization, is significantly – sometimes up to 5-10 times – higher than the latent heat of fusion. In vaporization, the change in density is however large, due to which the solid-liquid phase change process is preferred in TES applications.

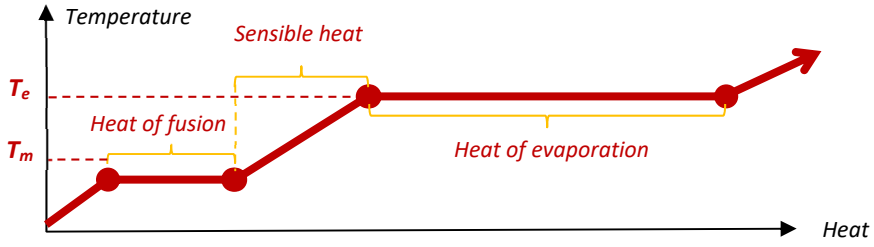

Figure 1: General heating curve for a material with phase changes: temperature as a function of heat added. T_m and T_e indicate the melting and evaporation temperatures, respectively.

PCMs are available from different groups of materials, both organic and inorganic, with a wide range of melting temperatures, energy densities, and other significant properties determining the applicability of the material. Classification of PCMs, their properties and selection of the correct PCM for a certain application is discussed in Section 2.

This report is written as a part the competence-building project PCM-Eff. The project, and thus the report, focuses on the utilization of LHTES in two particular applications: high-temperature LHTES for wood stoves, and low-temperature LHTES for refrigerated cabinets in food retail stores. In stoves, LHTES can increase the amount of energy utilized from the combustion process and help to avoid overheating and maintain the room temperature at the desired level over a longer period of time. In refrigerated cabinets, LHTES can help to maintain the product temperature at the desired level during power cut-offs and defrosting cycles. Utilization of PCMs in these particular cases is discussed in detail in Section 3. Keeping in mind these two applications, we have in this report chosen to define low-, medium- and high-temperature PCMs as follows:

- Low-temperature PCM: T_m varies from -30 to +4 °C
- Medium-temperature PCM: T_m varies from 10 to 80 °C
- High-temperature PCM: T_m varies from 80 to 600 °C

The primary drawback of most PCMs, apart from metallic PCMs, is their generally low thermal conductivity. A major challenge for systems employing PCMs is hence obtaining sufficient heat transfer between the PCM and the heat transfer medium, as well as within the PCM. Furthermore, some common PCMs are corrosive, which limits their application. Challenges related to enhancing the conductivity of PCMs and to PCM containment are discussed in detail in Section 4 of this report.

Proper designing of the TES systems using PCM requires quantitative information about heat transfer and phase change processes in a PCM [5]. For this purpose, models of the storage systems and simulations of their performance are beneficial to be able to efficiently make qualified predictions on the design, dimensioning and layout of storage units. Real world test rigs can be cost intensive and space demanding, and are locked to certain system specifications. With the help of a model, the dynamic behaviour of the system can be examined for several boundary conditions, and for different sets of system parameters [6]. Section 5 of this report is hence dedicated to the aspects of modelling PCM systems.

2 PCMs and their selection

PCMs are available from different groups of materials, with a wide range of significant properties determining the applicability of a material to a certain process. This chapter lists the important properties – thermo-physical and chemical properties, as well as those related to the economics and usability – and presents the most common groups of PCMs and their classification. Finally, a group of indicators that can be applied in selecting a PCM for a given process is presented.

2.1 Important PCM properties

Any candidate material to be used as PCM shall have first of all large latent heat and ideally high thermal conductivity. There is however no perfect PCM, and the choice of material is always a compromise. Often a PCM having some superior properties will also have some poor properties. Based on a survey of different studies, Oro et al. listed the main characteristics required for a useful PCM [7]:

- Thermo-physical properties:
  - Phase change temperature within the range appropriate to the application
  - Large latent heat per unit volume
  - Large sensible heat per unit volume
  - High thermal conductivity in both phases
  - Small volume changes due to the phase transition
  - Congruent phase change (no component segregation in the solid phase)
  - Sharpness of latent heat release and absorption: should occur over a narrow temperature range, depending on the application [8]
- Nucleation and crystal growth:
  - High nucleation rate (to avoid supercooling of the liquid during solidification and consecutive temperature hysteresis between solidification and melting)
  - High crystal growth rate (enabling fast charging/discharging of the PCM reservoir)
- Chemical properties:
  - Entirely reversible solidification/melting process
  - No chemical degradation with time and number of charging/discharging cycles
  - No corrosive properties to the construction/encapsulation materials
  - Non-toxic, non-flammable and non-explosive
- Economics and usability:
  - Easily available at low cost
  - Easily recyclable
  - Good environmental parameters based on Life Cycle Assessment

2.2 Classification of PCMs

PCMs can be categorized into organic, inorganic, metallic and eutectic PCMs, as shown in Figure 2. Organic, inorganic and metallic PCMs are discussed in the following sections. Eutectics are generally defined as alloys or mixtures exhibiting a distinct melting point for the whole mixture, which is lower than that of any

other alloy or mixture composed of the same constituents in different proportions. In the present context, the eutectic of interest is the mixture of salts and water, discussed in more detail in Section 3.1.1.

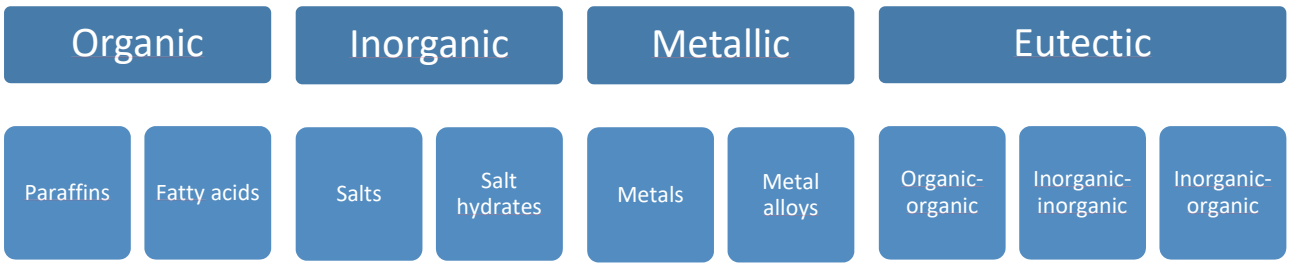

Figure 2: Classification of PCMs.

In addition, Figure 3 shows the temperature range and phase change enthalpy (latent heat of fusion) per unit volume for some of the common groups of PCMs. In Figure 3, it can be seen that salts, e.g. chlorides, carbonates and fluorides, have generally high melting temperatures and also high volumetric latent heats, owing to their high densities. Organic PCMs (paraffins and fatty acids) have relatively low melting temperatures, and the lowest volumetric latent heats of the PCM groups included in Figure 3. Metallic PCMs are not presented in this figure, however they are found in a wide range of melting temperatures and latent heats. Metallic PCMs are discussed in Section 2.2.3.

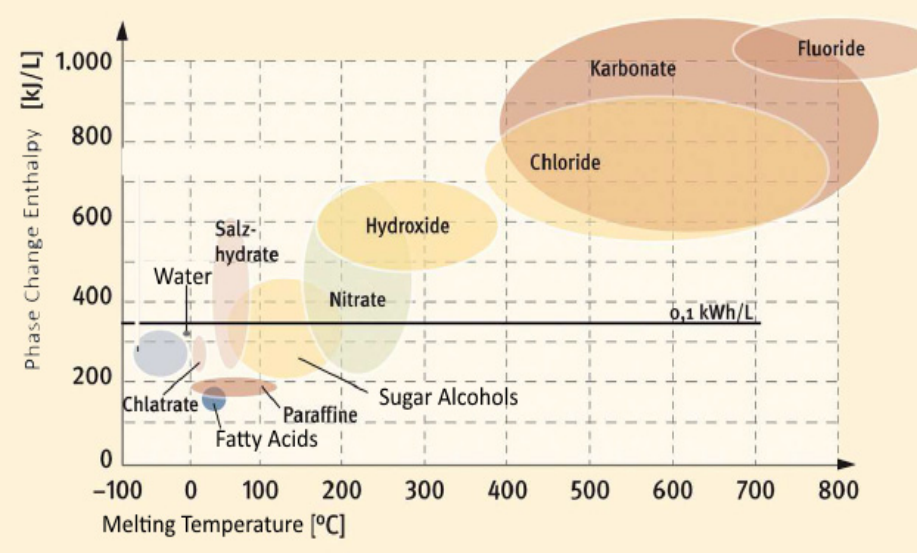

Figure 3: Temperature range and phase change enthalpy (latent heat of fusion) per unit volume for some common PCM groups [9].

2.2.1 Organic PCMs

Organic PCMs are among the most commonly applied PCMs, and include, among others, alkane (paraffin) (C_nH_{2n+2}) and fatty acids ($CH_3(CH_2)_{2n}COOH$) families [3]. They are suitable for medium temperature applications. Paraffins have melting temperatures ranging from 35 to 70 °C, and they are commonly used for thermal management in electronics. Fatty acids have lower melting temperatures, and are commonly used for applications related to thermal comfort, e.g., in residential buildings. Organic PCMs exhibit relatively high latent heats, in the range of 100-200 $kJ \cdot kg^{-1}$. They are physically and chemically stable, cheap, readily available, and easy to work with. However, their thermal conductivity is typically low (in the order of 0.2

$W \cdot (m \cdot K)^{-1}$), which limits their application. Furthermore, organic PCMs have relatively low densities and do not exhibit a sharp phase transition at the melting temperature but rather an extended transition taking place around the melting temperature. This is related to the fact that organic PCMs consist of large molecules including many compounds and molecules.

An emerging competitor for conventional organic and inorganic PCMs are vegetable-based PCMs. Fat- and vegetable oil-based PCMs with melting temperatures ranging from -90 to 150 °C and latent heats between 150 and 220 $kJ \cdot kg^{-1}$ have already been produced [8]. While e.g. paraffins are based on crude oil, vegetable-based PCMs make an entirely renewable, environmentally-friendly and safe product, and can often be locally derived using common agricultural crops, at low costs.

2.2.2 Inorganic PCMs

The most common, and undoubtedly the first PCM ever used, is water/ice, suited for keeping materials cold at around 0 °C. Water has a high latent heat of fusion, and is safe and easy to use. To lower the melting point, salts can be added to water. Eutectic salt solutions are discussed in more details in Section 3.1.1 in the context of low-temperature PCM applications. Comprehensive overviews of PCMs suited for cold TES, including different aqueous salt solutions are readily available in the literature [7].

Common inorganic PCMs for higher temperature applications include salts and salt hydrates. Salt hydrates are combinations of members of the inorganic salt families (oxides, carbonates, sulphates, nitrates and halides) with water molecules, following a specific ratio [3]. Salt and salt hydrates can be found with melting temperatures ranging from 10 to 900 °C. In the low temperature range, organic PCMs are preferred, but salts and salt hydrates are the most commonly applied PCMs in the high temperature range. Inorganic PCMs have sharp phase transitions at the melting temperature, latent heats comparable to those of organic PCMs, and higher thermal conductivities. Furthermore, they have higher densities, and exhibit smaller changes in volume during the phase change than organic PCMs. However, salts and salt hydrates tend to degrade over repeated thermal cycling, and are corrosive, hence not compatible with most materials. Moreover, they have a tendency for supercooling, meaning that the PCM might solidify at a temperature below the actual melting temperature. This problem can be tackled with adding nucleating agents into the PCM.

2.2.3 Metallic PCMs

Metals and metal alloys can be used as PCMs in both low, medium and high temperature ranges. Suitable metals for low-to-medium temperature applications include gallium and cesium with a melting temperature around 30 °C, and indium, tin and bismuth with a melting temperature around 100-200 °C [3]. For high temperature applications, from 400 to 700 °C, aluminium, zinc and magnesium can be used. Metals and metal alloys are the only groups of PCMs that do not suffer from low thermal conductivities, and most of them are safe and easy to work with. Their main drawbacks are their low latent heat and high density, which results in a high mass for the thermal storage. In the low-temperature regime, the latent heats of gallium and cesium are one order of magnitude lower than the organic PCMs with similar melting temperature. In the high-temperature ranges, however, metallic PCMs exhibit similar latent heats as salts and similar melting temperatures. Metallic PCMs are hence better suited for high temperature applications.

2.3 Selection of correct PCM

With a large variety of available PCMs, and a high number of properties affecting their suitability to a given application, the selection of an optimal PCM is not straightforward. This section details some key indicators to be used in the selection process of an optimal PCM, based on [10].

The analysis presented here is one-dimensional, and considers only conductive heat transfer. Convective effects can be significant with pure PCMs, however their relative importance becomes less significant with the inclusion of heat transfer enhancement (HTE), such as metal fins or foam (see Section 4.1). Furthermore, convective heat transfer adds substantial complexity in the models.

The first indicator is the energy density of the material, which should preferentially be high to store large amounts of energy in small volumes. A specific energy density is calculated from the heat of fusion and the sensible heat capacity from an ambient temperature T_{amb} up to the melting temperature T_m. Volumetric energy density, e_v [J·m^{-3}], is obtained by multiplying this with the material density:

$$e_v = \rho_s\left[c_p(T_m - T_{amb}) + H\right] \tag{1}$$

where H is the latent heat of fusion, and ρ_s and c_p are the solid state PCM density and specific heat capacity, respectively. The capacity of the heat storage and the incoming heat should be of the same order of magnitude:

$$e_v L \approx \Delta t_{cycle}\dot{q}_{hot} \tag{2}$$

where L is the storage thickness, Δt_{cycle} is the duration of the heating cycle, and $\dot{q}_{hot}$ is the average heat flux from the hot side [W·m^{-2}].

If the latent heat storage capacity of the PCM is low compared to the sensible heat storage capacity, the behaviour of the storage will be similar to the behaviour of a sensible heat storage. An important parameter is hence the ratio of latent to sensible heat capacity, C_r:

$$C_r = \frac{H}{H + c_p(T_m - T_{amb})} \tag{3}$$

This ratio is equal to 0 for a sensible heat storage, and 1 for melting temperatures equal to the ambient temperature. This ratio is particularly important for applications where the ambient temperature is far from the melting temperature.

The third indicator is related to the thermal conductivity. Fourier's law of heat conduction states that the local heat flux is equal to the negative temperature gradient multiplied by the thermal conductivity:

$$\dot{q} = -k_{eff}\frac{dT}{dx} \tag{4}$$

where k_{eff} is the effective heat conductivity, considering the effect of the HTE in the PCM. As thermal conductivities of PCMs are generally low, using a HTE is generally necessary (see Section 4.1). When fins are used as the HTE k_{eff} is calculated as:

$$k_{eff} = \varepsilon k_{PCM} + (1 - \varepsilon)k_{HTE} \tag{5}$$

where ε is the ratio of PCM volume to the total volume, and k_{PCM} and k_{HTE} are the thermal conductivities of the PCM and the HTE device, respectively.

For uniform temperature in the PCM and consequently uniform heat release, short distances between the PCM and the HTE, high k_{eff} as well as small thickness of the storage are required. The Biot number, *Bi*, is defined as the ratio between the external cold side thermal resistances (convective and radiative) and the internal conductive thermal resistance:

$$Bi = \frac{h_{cold} L}{k_{eff}} \tag{6}$$

where h_{cold} is the cold side heat transfer coefficient [$W \cdot m^{-2} \cdot K^{-1}$]. If the Biot number is large ($\gg 1$), the temperature difference between the hot and cold surfaces of the storage will be larger than the difference between the cold surface and the ambient temperature. This will then give a heat release similar to that of a sensible heat storage.

Finally, temperature degradation is a severe limitation in the use of PCMs. The temperature gap between the degradation temperature and the melting temperature, as well as the energy required to reach the degradation temperature should be large. An overheating indicator, describing how difficult it is to reach the critical temperature, can be defined as:

$$C_{crit} = \frac{H + c_{p,s}(T_m - T_{amb}) + c_{p,l}(T_{crit} - T_m)}{H + c_{p,s}(T_m - T_{amb})} \tag{7}$$

where $c_{p,s}$ and $c_{p,l}$ are the specific heat capacities for the solid and liquid phase, respectively.

The indicators given by Equations (1), (3), (6) and (7), i.e. the energy density, the ratio of latent to sensible heat capacity, the Biot number and the overheating indicator, describe the system of a PCM and the HTE and can be used to describe the performance of the latent heat storage. PCMs selected for a certain application from the basis of their melting temperature can then be ranked using these indicators.

3 Applications

3.1 Low-temperature

Typically, low-temperature (LT) thermal energy storage refers to processes occurring below room temperature, i.e., 20 °C [7]. Utilization of PCMs has been reported for various LT applications, such as protection of food and beverages, pharmaceutical products, blood derivatives, biomedical materials [7], as well as for air conditioning (AC) [11] and industrial refrigeration [12], [13]. For obvious reasons (low cost, good thermal properties, long stability and lack of toxicity), water is the most frequently used PCM in applications where the desired process or product temperature is close to 0 °C. Nevertheless, a wide range of PCMs has been evaluated for potential use in LT applications, with the main criterion of applicability being the phase change temperature.

3.1.1 Relevant PCMs for low-temperature applications

Relevant PCMs for LT energy storage include [7], [14], [11]:

- Organic PCMs: paraffins; alcohols and their aqueous solutions; alkanones; fatty acids and their mixtures
- Inorganic PCMs: water along with eutectic aqueous solutions of salts
- Eutectic PCMs: eutectic solutions of (typically) organic compounds, e.g., tetradecane + octadecane, pentadecane + heneicosane

The most frequently investigated and utilized low-temperature PCMs are shown in Table 1. Organic PCMs have self-nucleating properties but a lower thermal conductivity and higher capital costs. Inorganic substances are easily available at low cost but tend to exhibit component separation during phase transition and are often corrosive, as discussed in Section 2.2.2. In cases where eutectic materials are considered, components are mixed typically in the eutectic concentration at the eutectic point, namely congruent freezing with solid constant-composition mixture of both substances, free of component segregation [15], [11].

In addition to the different substances that have been studied for their potential utilization as PCM in cold storage applications presented in Table 1, a number of PCMs are commercially available, covering a wide range of melting temperature (between -50 °C and 18 °C) and heat of fusion (between 95 $kJ \cdot kg^{-1}$ and 386 $kJ \cdot kg^{-1}$) [11], [7]. The list of manufacturers contains among others Teappcm [16], Cristopia [17], Microtek Laboratories, Inc. [18], Rubitherm GmbH [19] and Climator [20].

In contrast to pure compounds and eutectic concentrations, non-eutectic concentrations (hypoeutectic and hypereutectic) lead to the phase transition occurring over a temperature range rather than at a single temperature, which may invoke non-uniform concentration profiles in the solid phase and consequent spatial discrepancies in physical properties of the solidified mass. Nevertheless, aqueous solutions of alcohols (mostly monoethylene glycol) are frequently used as PCMs with hypoeutectic concentrations [7], [21], for the temperatures limited to the area above the eutectic temperature. This ensures solidification of pure ice crystals from the concentrated solution (no component segregation in the solid). For monoethylene glycol, the eutectic point in the hypoeutectic region was experimentally determined to -49.9 °C at a glycol mass fraction of 0.58 [22].

Table 1: Thermo-physical properties of selected PCMs for LT TES, listed by phase change temperature.

Material	Type	Composition *(weight basis)*	Phase change temperature *(°C)*	Latent heat *(kJ·kg^{-1})*	Reference
2-Hexanone ($C_6H_{12}O$)	Alkanone	pure	-55.4	148.8	[12]
$CaCl_2/H_2O$	Aqueous solution of inorganic salt	0.298/0.702 (eutectic)	-55	164.93	[12]
***n*-Nonane (C_9H_{20})**	Paraffin	pure	-53.5	120.6	[12]
3-Heptanone ($C_7H_{14}O$)	Alkanone	pure	-37.1	153.5	[12]
2-Heptanone ($C_7H_{14}O$)	Alkanone	pure	-35.4	172.6	[12]
***n*-Decane ($C_{10}H_{22}$)**	Paraffin	pure	-29.6	201.8	[12]
***n*-Undecane ($C_{11}H_{24}$)**	Paraffin	pure	-25.5	141.9	[12]
Glycerol/Sodium formate/H_2O	Multicomponent organic	0.1/0.1/0.8	-23	174.5	[12]
$NaCl/H_2O$	Aqueous solution of inorganic salt	0.224/0.776 (eutectic)	-21.2	228.14	[12]
2-Octanone ($C_8H_{16}O$)	Alkanone	pure	-20.3	190.4	[12]
Ethylene glycol/Sodium acetate/H_2O	Multicomponent organic	0.1/0.1/0.8	-19	118.5	[12]
NH_4Cl/H_2O	Aqueous solution of inorganic salt	0.195/0.805 (eutectic)	-16	248.44	[12]
Ethylene glycol/Sodium propionate/H_2O	Multicomponent organic	0.1/0.1/0.8	-15	156	[12]
Glycerol/Sodium acetate/H_2O	Multicomponent organic	0.1/0.1/0.8	-14	127.8	[12]
Ethylene glycol/Sodium lactate/H_2O	Multicomponent organic	0.1/0.1/0.8	-12	157.4	[12]
KCl/H_2O	Aqueous solution of inorganic salt	0.195/0.805 (eutectic)	-10.7	253.18	[12]
Glycerol/Sodium lactate/H_2O	Multicomponent organic	0.1/0.1/0.8	-10	159.3	[12]
***n*-Dodecane ($C_{12}H_{26}$)**	Paraffin	pure	-9.5	216.2	[12]
***n*-Tridecane ($C_{13}H_{28}$)**	Paraffin	pure	-5.3	154.5	[12]
5-Nonanone ($C_9H_{18}O$)	Alkanone	pure	-3.8	175.3	[12]
NaF/H_2O	Aqueous solution of inorganic salt	0.039/0.961 (eutectic)	-3.5	314.09	[12]
Na_2CO_3/H_2O	Aqueous solution of inorganic salt	0.059/0.941 (eutectic)	-2.1	310.23	[12]
H_2O	Water	pure	0.0	333	[12]
$C_{13}H_{28}/C_{14}H_{30}$	Paraffin mixture	0.2/0.8	2.6	212	[14]
$Na_2SO_4/NaCl/KCl/H_2O$	Aqueous solution of inorganic salts	0.31/0.13/0.16/0.4 (eutectic)	4	234	[7]
$LiClO_3{\cdot}3H_2O$	Inorganic hydrated salt	pure	8	253	[7]

When selecting the correct PCM for given cold storage applications, detailed phase equilibrium information expressed as a phase diagram becomes vital since in many applications the exact range of the PCM phase change temperature is not known a priori. Thus, combining the expected process temperature

range with the specific PCM phase diagram enables a more accurate evaluation of the thermal storage density available for the considered PCM [7].

3.1.2 Practical challenges

A number of practical challenges have been reported while using various PCMs, namely phase segregation, supercooling, toxicity, flammability and corrosion. Most of them could be dealt with by the use of relevant additives to the PCM mass.

3.1.2.1 Phase segregation

Phase segregation, or incongruent freezing/melting, is mostly related to inorganic non-eutectic mixtures. It can lead to inefficient solidification and melting processes. This issue can be addressed by adding water with thickening or gelling agents. Thickening increases the solution viscosity so that both components are held together. Similarly, by adding gel as a crosslinked material to the salt, a three dimensional network that holds the salt solution together is created [12].

3.1.2.2 Supercooling

The phenomenon of supercooling (often inappropriately called subcooling) occurs when the start of solidification suffers from a temperature offset (called supercooling degree). This can be handled by adding nucleating agents, by using cold fingering method (local boosting of supercooling degree by the use of auxiliary cooling devices or agents) and by exerting physical fields (ultrasonic field, electromagnetic field, magnetic field, etc.) to boost the rate of homogeneous nucleation. Good examples of nucleating agents for aqueous solutions are carbon nanofibers, copper suspension, titanium oxide as well as potassium sulphate and borax [12]. The hexagonal structure of the silver iodide crystals resembles closely the structure of ice crystals and was found a very effective nucleate agent for mixtures of water and salts [21], [12]. Other effective nucleating agents for aqueous solutions are e.g. $BaCO_3$, $BaCl_2$, BaI_2, $Ba(OH)_2$, CaC_2O_4, K_2SO_4, $MgSO_4$, $SrCl_2$, $SrCO_3$, $SrSO_4$, $Sr(OH)_2$, TiO_2 [12].

Surface roughness is another important factor influencing heterogeneous nucleation, namely, higher roughness for the heat exchanging surface increases the rate of heterogeneous nucleation.

3.1.2.3 Long term and cyclic stability, and corrosion

Poor stability of the materials properties and/or corrosion are the main factors responsible for degradation of the PCM-based energy storage devices. Based on the results of thermal cycling tests, stainless steel was identified as the most corrosion resistant for use with aqueous solutions of salts and salt hydrates [7], [12]. Another solution used very often in practice is encapsulation (see section 4.2), acting as barrier to protect from mutual corrosive interaction between the PCM and container material.

3.1.2.4 Toxicity

Toxicity represents a potential issue in cases where the PCM might be in contact with food or operators, for example. In such cases, either the toxic PCM could be simply avoided and replaced by another PCM, or PCM encapsulation (see Section 4.2) could solve the issue by isolating the PCM from the surrounding. Another aspect to consider regarding toxicity is the impact on the environment, especially if the PCM does not present a long-term stability and should be replaced often.

3.1.2.5 Flammability

In applications where the LHTES system is not fully contained or might be exposed to fire risks (e.g. technical room of an office building, high-temperature processes), the PCM properties should be thoroughly investigated regarding flammability. For PCMs such as paraffins, their high flammability might limit their application.

3.1.3 Examples of PCM applications at low temperatures

3.1.3.1 Cold storage in air conditioning and free cooling

LHTES can be installed in an air conditioning (AC) system, either in a chilled water circuit, ventilation system, or in the thermal power generation of desiccant cooling and absorption systems [11]. The potential benefits of using PCMs are: peak-load shaving, potential reduction of the overall size of the installed machinery, as well as better use of the installed power at part-load.

A cold-storage accumulation tank for peak-load shaving installed in a traditional fan-coil chiller system has been presented and evaluated by De Falco et al. [23]. A 5-kWh prototype storage tank, with a PCM inlay based on a heterogeneous (immiscible) mixture of RT5HC by Rubitherm GmbH and water, was modelled and tested experimentally for a 5.7 kW AC system. The melting temperature of the PCM was 5.5 °C while latent heat of fusion was 240 kJ·kg^{-1}. The PCM, having lower density than water, is located in the upper part of the storage tank while water is recirculated by a circulation pump through the inner tube of the tube-in-tube heat exchanger (see Figure 4). The PCM inlay exchanges heat not only with the primary circuit through the wall of the outer tube of the heat exchanger, but also with a secondary circuit through water droplets falling on the PCM bulk. Moreover, the water jets enhance the circulation of liquid PCM, thus improving the heat transfer in the PCM bulk even more. It was found that the storage tank could be fully charged in 54 minutes.

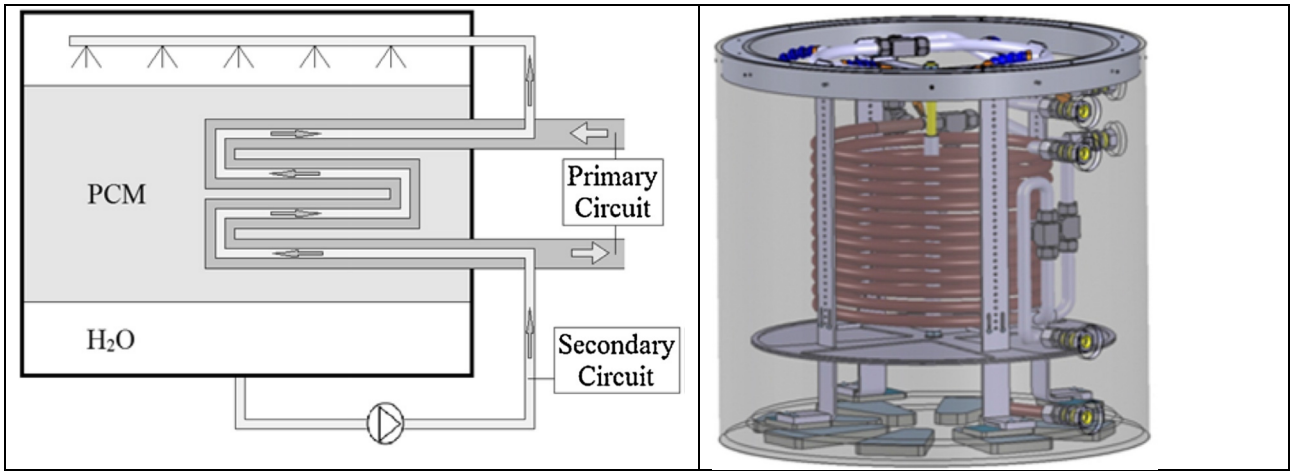

Figure 4: Cold storage tank with primary and secondary circuits for heat transfer intensification [23].

Raj and Velraj [24] have designed and investigated, both numerically and experimentally, a regenerative PCM shell-and-tube heat exchanger incorporated into a ventilation system for free cooling purposes. During the night time, the low-temperature ambient air was used to charge the PCM modules, while, during the day time, the warm room air is cooled down by circulation through the PCM modules (see Figure 5). The PCM modules of the modular heat exchanger are stacked one on top of each other with air spacers in between

each module. A paraffin PCM with a latent heat of fusion of 82.7 kJ·kg^{-1} and a melting temperature in the range 24 - 28 °C was used. The main findings were that the air spacers provided between the modules improved the heat transfer and their effect was more pronounced at lower velocities and decreased as the inlet velocity increases. Their effect is negligible above an inlet velocity of 2 m·s^{-1}.

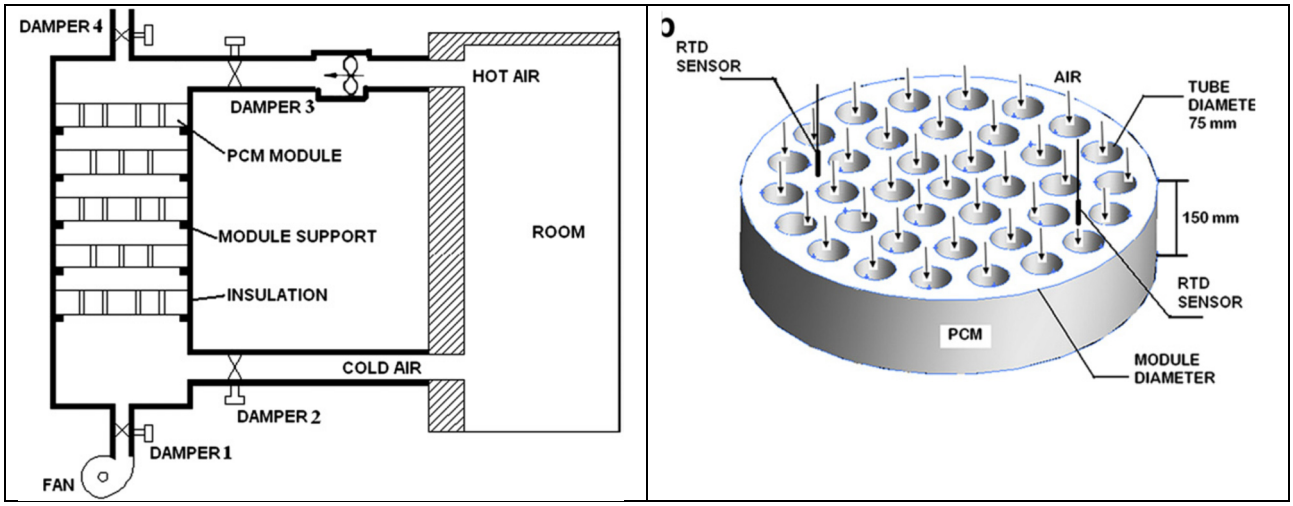

Figure 5: Operation of the free cooling system and structure of a single PCM module [24].

3.1.3.2 Food storage

One of the most common applications of PCMs is transportation of temperature-sensitive foodstuff in refrigerated containers, equipped with an internal chiller or cooled down periodically with an external system [7]. Nevertheless, a field that has gained much attention in the recent years is stationary PCM-supported systems for cold storage rooms or refrigerated display cabinets.

Lu et al. [25] have developed a novel design for an open-type refrigerated display cabinet where PCM-supported storage shelves were used to improve the temperature uniformity during defrosting periods. It was discovered that the new shelf design with the PCM inlay and heat pipes for heat transfer enhancement reduced the food temperature by 1.5 °C during defrosting periods and ensured a more uniform product temperature, compared to the original non-modified cabinet. All the effects were recorded without energy penalty, i.e., the energy consumption of the whole cabinet remained basically unchanged.

Lu and Tassou [21] investigated experimentally various candidate PCMs for application in chilled refrigeration cabinets for a product temperature range between 0 °C and +5 °C. The results showed that paraffins exhibited negligible supercooling but have low latent heat compared to water-based mixtures that, on the other hand, are burdened with a greater supercooling. Water-based polymer gels with addition of silver iodine as nucleate agent proved to supress the supercooling effect significantly. The main conclusions were as follows:

- The minimum temperature difference between the PCM and the heat transfer fluid required to initiate freezing was 1.5 K for water gels and 2.5 K for water/glycol mixtures; the required temperature difference during melting was slightly lower, i.e., 1 K.
- For applications where the requested phase change temperature is 0 °C, water gel with silver iodine (with concentrations higher than 1.6 %) could be applied to obtain a heat transfer fluid temperature below -1.4 °C / above 1 °C for freezing/melting, correspondingly.

- For applications where the requested phase change temperature is lower than 0 °C, water/antifreeze gel with silver iodine (with concentrations higher than 2.5 %) shall be used; for example, a 10 % water-propylene glycol solution (with equilibrium phase change temperature of -3 °C) gives a heat transfer fluid temperature below -4.3 °C / higher than -2 °C for freezing/melting, correspondingly.

Alzuwaid et al. [15] investigated experimentally the performance of a refrigerated open-type multi-deck display cabinet with integrated PCM inlays, placed into two single-panel fin radiators for efficient heat exchange (see
Figure 6). The water-based gel PCM was composed of deionised water as the phase change agent, 1.2 % silver iodide for supercooling suppression, and 0.9 % of guar and 0.15 % of sodium tetraborate for gel cross-linking, resulting in freezing onset at around -2 °C. The cooling load and effective defrosting time were estimated to 2.24 kW and 4 minutes, respectively, while the overall amount of PCM in the radiators was 1.86 kg. The display cabinet, with and without integrated PCM inlay, was tested experimentally in a climate chamber (for climate class 3 according to the BS EN ISO 23953-2: 2005 standard) for performance comparison. The 24-hour long tests showed that, by installing the PCM radiators, up to 5 % of energy savings could be registered. The defrosting time was extended from 7 min to 12 min, while the maximum air temperatures in the cabinet were reduced by 2 K. The product temperature was reduced on average by 1 K.

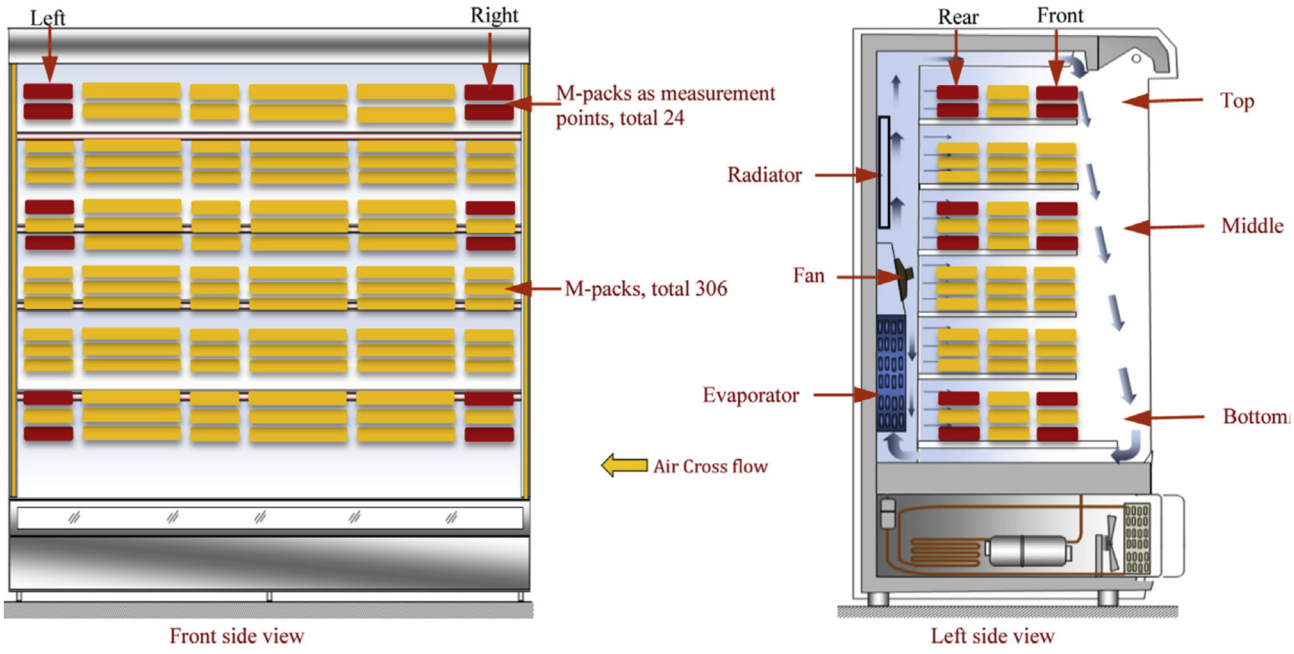

Figure 6: Layout of the PCM-supported refrigerated cabinet tested by Alzuwaid et al. [15].

Alzuwaid et al. [26] developed and experimentally validated a 2D CFD model of a prototype open-type multi-deck refrigerated display cabinet with integrated PCM inlay, used previously in the tests reported in [15]. For the experimental setup and test conditions, the authors concluded that:

- The maximum air temperatures in the original cabinet (without PCM inlay) are higher, while the minimum temperatures are lower, as shown in Figure 7.
- Due to the reported extension of duration of both short cycles and long cycles, the number of short cycles was reduced from 11 to 8 (counted for a 4-hour period between the defrosting cycles, see Figure 7). Short cycles result from the thermostat cut-off temperature setting, controlling the actual value of the return air temperature, i.e., temperature of air flowing back to the evaporator. Long

cycles result from controller settings for defrosting cycles for periodic removal of frost from the evaporator surface.

- Energy savings in the energy consumed by the compressor, counted for a 36-min period, were registered for the cabinet with PCM (see Table 2).
- For the modified cabinet, the whole range of product temperature is more moderate than that without PCM, resulting in better temperature uniformity.
- An optimization procedure is required for the PCM inlay design (mostly for the overall mass of the PCM), taking into account the cabinet size, rated working conditions (indoor space air temperature and relative humidity), and initial design of the cabinet (air distribution, regulation/defrosting strategy, etc.).

Details regarding the modelling work in the study by Alzuwaid et al. [23] are given in Section 5.4.2.

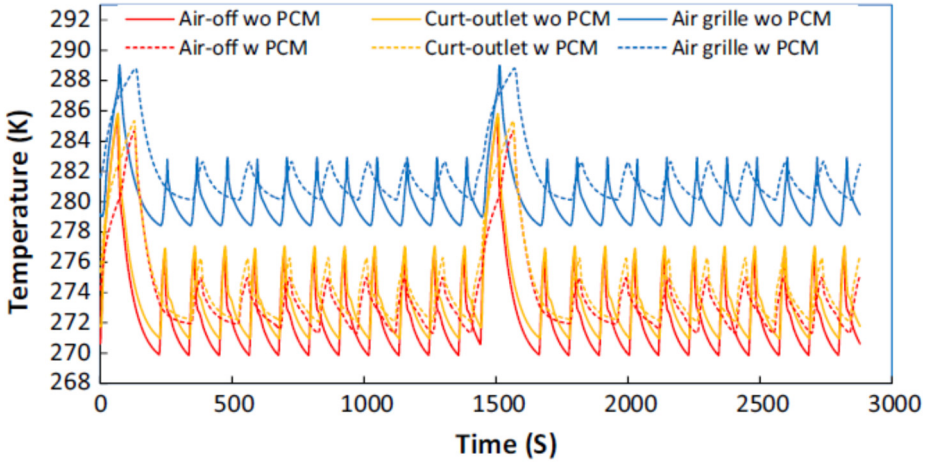

Figure 7: Variations of cabinet air temperatures with time, with and without PCM [26].

Table 2: Energy consumption parameters for a cabinet, with and without PCM inlay [26].

Energy parameters	Without PCM	With PCM
Average compressor power *(kW)*	1.6	1.6
Overall run time *(hours)*	0.6	0.6
Overall 'on' time *(hours)*	0.4875	0.45
Overall 'off' time *(hours)*	0.1125	0.15
Overall energy consumption *(kWh)*	0.78	0.72
Number of compressor starts	72	54
Energy savings	-	6.4 %

3.2 High-temperature

The high-temperature (HT) range is, in the present report, defined from 80 °C to 600 °C. Between 20 °C and 80 °C, applications are today well understood and many commercial solutions are available. This applies especially in the building industry and for thermal management of electronic equipment. Above 600 °C, fewer applications exist and various technical challenges arise. Due to the high potential for PCMs with high melting temperature up to 900-1000 °C to store energy in solar concentrating technologies, properties for such PCMs can be found in the literature [1, 2, 27]. Beyond this temperature, the literature is scarce. For the HT range

from 80 °C to 600 °C, several thorough reviews are available [4, 27-30], though the listed PCMs in the literature for the HT range often lack accurate physical properties data (e.g., thermal conductivity for both liquid and solid phases, melting temperature range).

The HT application of highest interest in the present report is for wood stoves. In such stoves, a large amount of heat is released from the stove surfaces and the stovepipe to the ambient during the combustion phase. E.g., PCMs surrounding the stovepipe could enable an increased utilization of the generated heat and a more even heat release from the stove over an extended time. Applications of PCMs in wood stoves have rarely been studied [10, 31, 32].

3.2.1 Relevant PCMs for high temperature applications

Considering the very large temperature range considered for the HT applications, examples of PCMs have been gathered in Appendix A.

Haugen [33] evaluated PCMs applicable for heat storage associated to wood stoves and found that the sugar alcohol erythritol and the molten salt sodium acetate trihydrate are the most promising. Both are commercially available and their relevant properties are summarized in Table 3.

Table 3: Thermo-physical properties for sodium acetate trihydrate and erythritol [33].

Properties	Sodium Acetate Trihydrate	Erythritol
Melting temperature *(°C)*	58	118
Degradation temperature *(°C)*	115	160
Melting heat *(kJ·kg^{-1})*	260 ± 11	339.8
Specific heat capacity (liquid) *(kJ· (kg.K)$^{-1}$)*	3	2.76 (at 140 °C)
Specific heat capacity (solid, 20 °C) *(kJ·(kg·K)$^{-1}$)*	2.79	1.38
Conductivity (liquid) *(W·(m·K)$^{-1}$)*	0.4	0.326
Conductivity (solid, 20 °C) *(W·(m·K)$^{-1}$)*	0.7	0.733
Density (liquid) *(kg·m^{-3})*	1280	1300 (at 140 °C)
Density (solid, 20 °C) *(kg·m^{-3})*	1420	1480

Agyenim et al. [34] reviewed PCM materials investigated over three decades, and presented thermo-physical data for a range of typical and relevant PCMs studied or proposed for study by previous authors. Properties for PCMs with melting temperature between 100 °C and 300 °C as summarized by Agyenim et al. are presented in Table A.1 (Appendix A).

Pereira da Cunha et al. [35] reviewed low and medium temperature applications using PCM and found that organic and salt hydrates seemed more promising for phase change temperatures below 100 °C and eutectic mixtures from 100 to 250 °C. Properties for some of the PCMs with melting temperature between 80 °C and 250 °C and with relatively low price as summarized by Pereira da Cunha et al. are presented in Table A.2 (Appendix A). Due to the lack of experimental data for some of the thermo-physical properties of eutectic mixtures, some of the missing values were evaluated by Pereira da Cunha et al. using weighting methods.

Due to the scarcity of pure-component melting points between 300 °C and 500 °C, it seems that multicomponent PCMs are required for this temperature range [36]. A review of PCMs with melting

temperatures above 300 °C was performed by Liu et al. [29]. Properties for PCMs with melting temperature between 300 °C and 600 °C as summarized by Liu et al. are presented in Table A.3 for inorganic substances, in Table A.4 for inorganic eutectics and in Table A.5 for metals and metal alloys (Tables available in Appendix A).

The commercial PCM manufacturer EPS Ltd (epsltd.co.uk) offers many PCMs with melting temperatures in the range -100 to 885 °C through their platform PCM Products Ltd. (pcmproducts.net). On their website, the PCMs are listed with corresponding thermo-physical properties (phase change temperature, heat of fusion, density, volumetric heat capacity, specific heat capacity, thermal conductivity and maximum temperature).

3.2.2 Practical challenges

Practical challenges with most PCMs at medium to high temperatures include phase segregation, supercooling and long-term and cyclic stability and corrosion. The relative importance of these challenges depends on the PCM nature and composition: for example, salt hydrates are known for their corrosive properties, while sugar alcohol can be subject to supercooling. Metals, in comparison, do not present such challenges though their high density is generally a limiting factor for their deployment as PCM. In general, all of the mentioned aspects should be thoroughly evaluated with regards to the considered application and containment method.

In addition, a known practical challenge at higher temperatures is the thermal degradation of the PCM. The latter challenge typically occurs when the PCM is heated up to temperatures significantly higher than its melting temperature. When used for wood stoves for example, the PCM temperature varies from room temperature to several hundred degrees, where the highest temperatures are highly dependent on the wood stove operator's control of the heat production [10]. Thermal degradation will affect the PCM properties (e.g. latent heat of fusion, phase segregation) and usually reduces its capability to achieve the task the thermal energy storage unit was designed for. Ideally, either the temperature domain between melting and degradation temperatures shall be large or the system shall prevent reaching the degradation temperature. Another challenge associated to thermal degradation is the lack of reliable data about thermal degradation temperature for some PCMs.

Another form of thermal degradation is the thermal decomposition of salt hydrates, such as $MgCl_2.6H_2O$ for example. The latter dehydrates as the temperature rises above the salt melting temperature. The reaction equation below shows the principle [37]:

$$\text{Salt} \,.\, x\text{H}_2\text{O}_{(\text{s})} + \text{Heat} \leftrightarrow \text{Salt} \,.\, (x-y)\text{H}_2\text{O}_{(\text{s})} + y\text{H}_2\text{O}_{(\text{g})} \quad (8)$$

The reaction above is in theory reversible. However, the reversibility of the reaction will depend on the design of the LHTES system, since it involves mixing of solid and gas phase and a potential leakage of the gas. Literature can be found on the characterisation of the thermal decomposition of most usual salt hydrates. It should also be noted that thermal decomposition can be used as a thermochemical heat storage system, provided a specific design [37] to ensure reversibility.

3.2.3 Examples of LHTES applications at medium to high temperatures

Medium- to high-temperature PCM systems are today found throughout a wide range of applications, subdivided into two main categories: thermal management and latent heat thermal energy storage (LHTES).

Thermal management relying on PCM systems is generally found in power electronics to reduce the temperature increase rate near the threatened components thanks to the latent heat properties [38]. Electronic components work best within a short range of temperatures though they are exposed to either large and predictable variations of temperatures or punctually elevated temperatures. PCMs yield a buffering effect of the generated heat, which is applied especially successfully with devices with intermittent usage patterns, such as mobile phones [39]. Though out of the scope of the present report, thermal management using PCMs greatly contributed to the research on PCM properties and PCM commercialisation at large scale.

LHTES systems have been mostly studied and to some degree applied in the following areas:

- Building materials and technologies
- Concentrated solar power (CSP) plants
- Excess heat recovery and utilisation in industry
- Passive temperature regulation for transportation (including space applications).

Since LHTES applied to wood stoves is the main area of interest for the present report within this temperature range, it is also presented in this Section, though the literature in this field is still scarce.

3.2.3.1 Building applications

In buildings, LHTES is used, for example, to increase thermal comfort, provide passive heating or cooling and enable use of solar thermal heating. They are found in e.g., air-conditioned units, wall and roof materials, and solar thermal units. Some passive systems rely for example on daytime/night time temperature variations. Most applications rely on PCMs with phase change at ambient temperatures or under 80 °C, thus they are out of the scope of the present report. A number of complete reviews of such applications can be found in the referred literature [40-43].

As an example of application, Al-Abidi [44] reported on a successful numerical and experimental study of a LHTES system applied to a liquid desiccant air-conditioning system. The study relied on a triplex tube heat exchanger with internal and external fins, where the PCM was enclosed between the two tubes (see Figure 8). The PCM was RT82, commercially available from Rubitherm GmbH-Germany [45] and with phase change in the range of 77-85 °C.

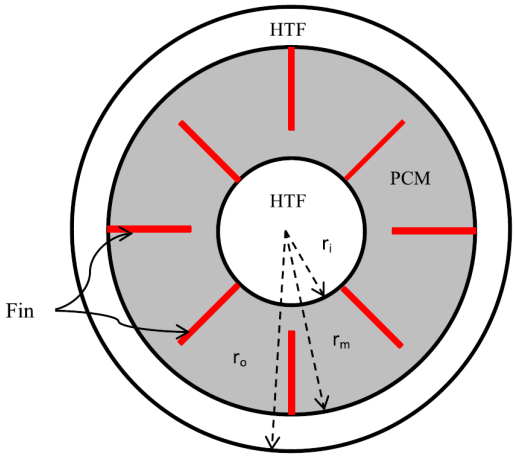

Figure 8: Geometry of the triplex tube heat exchanger studied by Al-Abidi [44].

3.2.3.2 Concentrated solar heat

Applying PCMs in concentrated solar power (CSP) plants has received a lot of attention in the last decade due to the cyclic and intermittent nature of the solar radiation. PCM for such applications are typically inorganic salts and metal alloys with melting temperature from 120 °C to 1000 °C [2]. Properly designed LHTES systems yield more compact storage tanks leading to significant reduction in space demand and construction costs [46]. Solar power plants can aim at direct steam generation and generate electricity through steam turbines. The most known and mature CSP technologies are parabolic trough, solar tower, linear Fresnel and Dish-Stirling. Parabolic trough technologies are commercially available and most widespread. Their capacity is rarely above 50 MW_{el} and their annual solar-to-electricity net efficiency is within 11-16 % [47].

Hoshi et al. [2] studied a power plant integrating high-temperature LHTES storage as shown in Figure 9. Provided a high melting temperature, using PCM would significantly increase the overall system efficiency through the preheating of the process water upstream from the boiler.

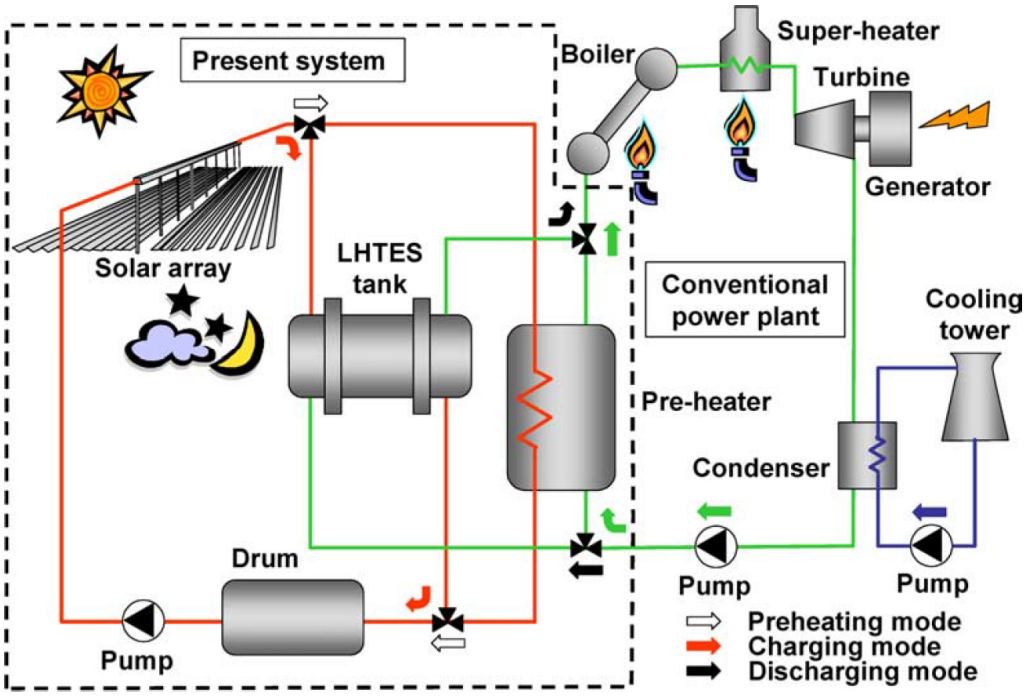

Figure 9: Power plant design integrating high-temperature LHTES storage [2].

3.2.3.3 Excess heat recovery and utilisation in industry

Among the many solutions studied to recover excess heat in industrial processes, LHTES is very promising [48] to achieve both energy savings and lower CO_2 emissions. For example, Steinparzer et al. [49] numerically analysed the heat recovery from intermittent exhaust gas of an electric arc furnace from a steelmaking industry with molten salts, among other TES systems. Out of the estimated excess heat production of 370 kWh per ton of liquid steel, up to 24 % could be recovered in the exhaust gas, stored and contribute to continuously generate process steam or electricity on-site. Therefore, energy consumption could be reduced by 60-80 kWh per ton of liquid steel, and CO_2 emissions could be reduced by up to 45 kg per ton of liquid steel.

Miro et al. [48] reviewed TES solutions for various types of industries in a comprehensive study. The authors also focused on the particular case of off-site excess heat utilisation. Methods of heat distribution through pipelines such as with district heating, within an industry cluster or a city-level, are a prerequisite for this. However, in remote places where the heat demand density is insufficient to justify the required investment and maintenance of a district heating network, mobilized-TES can be a viable option. The following aspects should be considered to optimize mobilized-TES: high energy density, high charging and discharging energy rates, temperature stability with regards to the container and suitable operational strategy. A number of findings are given below, based on the survey by Miro et al. of the literature on mobilized-TES applied in Germany, Sweden and Japan:

- Steelworks, aluminium factory/incineration, CHP plants and incinerator plants are relevant candidates to collect industrial excess heat.
- Sources of excess heat are favoured in the form of exhaust gas at temperatures in the range 70 – 350 °C, preferably above 200 °C. Within this range, most studies pointed towards TES materials such as zeolite, sodium acetate trihydrate, erythritol, sodium carbonate and sodium hydroxide, most of which are used as PCMs.
- The TES material shall amount to 14 – 17.5 tons to offer a sufficient and significant storage capacity of up to 2 to 3 MWh.
- On the demand side, various options have been studied, such as utility plants, industrial drying processes, air conditioning, swimming pools, district heating networks and chemical plants.
- Distances between heat source and heat sink in the surveyed studies were generally kept within 20 km maximum to realise consequent energy savings and CO_2 emissions abatement in the range of 70 – 95 %.
- The general rule of thumb remains: the shorter the distance between heat source and heat sink, the higher the energy saving and the higher the CO_2 abatement.

3.2.3.4 Passive temperature regulation for transportation

An interesting area of applications to be mentioned is thermal buffering for motor vehicles, thoroughly reviewed by Jankowski et al. [50]. Most vehicle components must be able to operate from sub-freezing temperatures up to peak temperatures of several hundred degrees Celsius [51]. To be viable for implementation in vehicles, a PCM system should then enable to, e.g., replace existing components, protect key electronic components, improve overall efficiency, downsize systems and extend lifetime of components. The direct applications can be grouped by temperature range:

- Below 100 °C, applications are related to, e.g., energy storage for cold start improvement, indoor climate system thermal buffering, air conditioning systems, electronics thermal management, vehicle battery thermal buffering.
- At temperatures between 100 and 200 °C, applications are related to, e.g., engine coolant loop thermal buffering and power electronics thermal buffering.
- At temperatures higher than 200 °C, applications are related to, e.g., exhaust gas energy recovery, cold start buffering and catalytic converters.

3.2.3.5 TES associated to wood stoves

With a large variety of available PCMs, and a high number of properties affecting their suitability to a given application, a method was developed to assist the selection process of an optimal PCM for LHTES with wood stove combustion based on a one-dimensional analysis providing key indicators [10]. The method is detailed in Section 2.3. The performance of the LHTES is described through the energy density, the ratio of latent to sensible heat capacity, the Biot number and an indicator of overheating risk. These indicators allow effective ranking of PCMs selected for a given application.

Various studies investigated the opportunities for thermal energy storage associated to wood stoves. Benesch et al. developed a CFD-based methodology for the analysis and optimization of a wood log stove with a sensible heat storage device [52]. The results enabled to test different storage materials in solid state. The same group also developed guidelines for heat storage units based on phase change materials, still addressing wood stoves [31]. It was notably pointed out that the PCM melting temperature should not be too high to allow charging at partial combustion load. The following criteria were listed as the most important and challenging: low flammability, low thermal degradation, high heat capacity, high density, suitable melting temperature, affordability, low corrosivity and low toxicity. The advised approach in the guidelines was however the full integration of the PCM in the side wall(s) of the stove allowing the flue gas to circulate through the PCM and to discharge heat with the assistance of air channels and free convection. This approach allows to increase the heat release rate. Figure 10 shows an example of such an implementation, which was successfully numerically and experimentally tested and shall in theory be introduced to market within 2018-2019 [53]. The results, however, point out the presence of very large temperature variations within the PCM, which requires a careful selection of material as PCM to avoid reaching its degradation temperature.

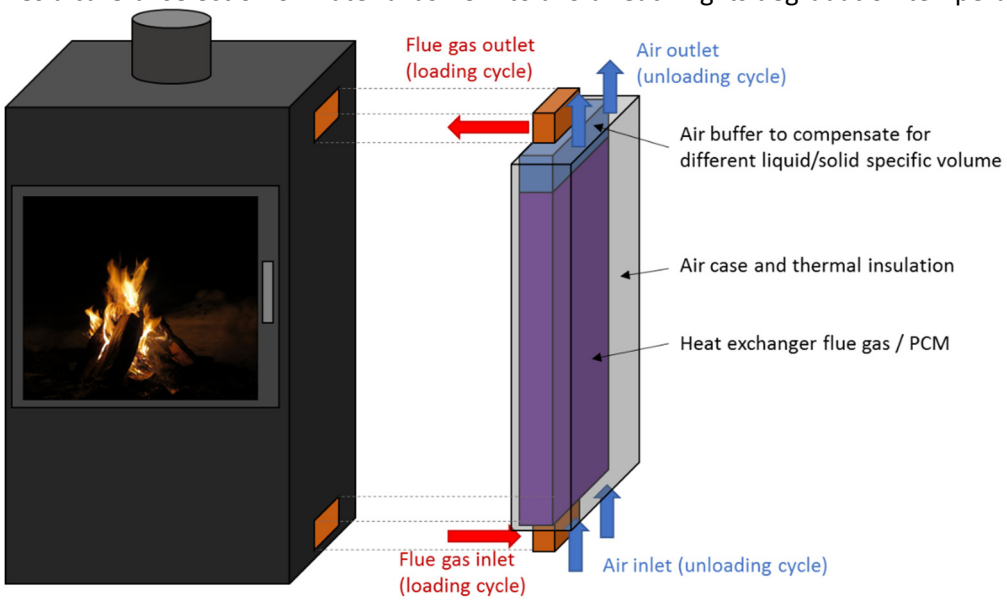

Figure 10: Implementation of a LHTES units on the side of a wood stove as investigated by Obernberger et al. [53].

A study by Zielke et al., involving a wood stove manufacturer, similarly focused on the technical design and construction of a stove surrounded by plates filled with salt hydrates melting at 60 °C [32]. The goal was to avoid firing the stoves at partial load during night and the associated high emissions, while maintaining the heat comfort. Though the results proved positive, the solution has not yet been commercialized due to the difficulty to achieve a commercial design in line with the customers' expectations. This outcome points out one key challenge in commercialising a TES solution for wood stoves, where the aesthetics may play a role at least as important as performance.

4 PCM design challenges

4.1 Enhancement of thermal conductivity

One of the most significant barriers to large-scale deployment of PCM-based thermal energy storage units is the generally low thermal conductivity of PCMs [3]. Low thermal conductivity may cause the PCM to act as a thermal insulator rather than a thermal sink. This issue is critical in applications where the available thermal charging time of the PCM is shorter than a few hours, which is a typical time frame of complete phase change for a PCM system.

During melting, in applications where the thermal source temperature is significantly higher than the PCM phase change temperature, low thermal conductivity of the liquid PCM may cause overheating of the first layer of melted PCM instead of transferring heat further into the PCM mass.

During solidification, conduction dominates the heat transfer. A low thermal conductivity of the solid PCM may affect the heat flow negatively, potentially resulting in the layer of PCM closest to the heat sink solidifying and creating a thick layer of low thermal conductivity isolating the remaining liquid away from the heat sink.

Several solutions are available to enhance the effective thermal conductivity and speed up the phase change processes without significantly impacting the heat storage capacity of the PCMs storage container:

- Metallic inclusions
- Macroscale or nanoscale carbon inclusions
- Heat pipes

The following sections provide details and key aspects on these methods, based on a review written by Fleischer [3].

4.1.1 Metallic inclusions

Embedding metallic inclusions improves significantly the effective thermal response in the PCM mass, due to the higher thermal conductivity of metals. Two main designs are to be considered: metallic fins and metallic foam inclusions.

4.1.1.1 Metallic fins

Embedding fins connected to the heat sink or heat source within the PCM container enables to effectively speed up the heat transfer along the path created by the fins, and increasing the heat transfer surface area. Another positive aspect of the fins is that they divide the PCM mass into smaller cells, enhancing the overall heat diffusion and phase change. The fin orientation shall preferentially take into account its effect onto natural convection in the liquid phase, so that the fins contribute to homogenous phase change conditions in the PCM.

The dimensions or the number of the fins do not have to be large to be effective, especially since the volume of fins naturally impacts the effective heat capacity of the PCM systems. Various numerical and experimental studies have looked at the influence of the fin dimensions onto PCM systems [54-57]. Most of

them agree that, considering internal fins connected to the heat source, the heat penetrates quickly along the length of the fin and then into the PCM, with a much lower proportion of the heat moving directly from the heat source interface into the PCM. As shown in Figure 11, with a large space between parallel fins, the melting front moves away from each fin plate towards the next fin plate. With smaller distance between the fins, the melting front at the heat source interface, perpendicular to the fins, is significantly accelerated (right side in Figure 11).

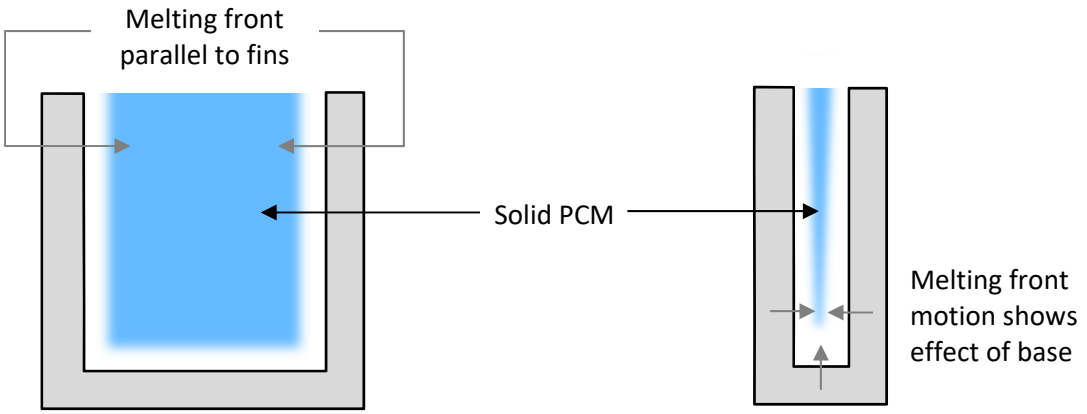

Figure 11: Melting front motion between fins. Left: Parallel for widely spaced fins. Right: Impacted by baseplate melting for tightly spaced fins [3] (redrawn).

Another way of considering this aspect is to investigate the effect of the aspect ratio of the plate fins, defined here as the fin height divided by the distance between the fins [55]. A large aspect ratio reflects tall and tightly packed fins, while a small aspect ratio features short and widely spaced fins. The low aspect ratio designs were found to dissipate most of their heat through the baseplate with the melt front almost parallel to the baseplate, while the high aspect ratio designs were found to be conduction dominated due to the extremely thin PCM layers.

Some key disadvantages of embedded metal fins include: added weight, and more importantly, displacement of PCM volume, reducing the effective specific heat capacity in the energy storage container.

4.1.1.2 Metallic foam

Metallic foam has been investigated to solve the above-mentioned disadvantages by featuring larger surface area per volume and hence improving the effective thermal conductivity and diffusivity within the PCM mass. Similarly to metallic fins, the heat flows along the metallic foams, separating the PCM into smaller cells. Various metals have been investigated experimentally and numerically for metallic foams, most commonly aluminum [58], as well as copper [59] and nickel foams [60]. Due to their high thermal conductivity, metallic foams enable to reduce the temperature variations throughout the PCM mass and hence contribute to more uniform melting or solidifying process.

Using a metallic foam featuring high porosity eventually leads to a conduction-dominated heat transfer, nearly suppressing natural convection, though still presenting a better overall thermal performance than without the metallic foam. During solidification, which is conduction dominated, using metallic foam will decrease the solidification time. One study measured effective thermal conductivities for copper foams filled with paraffin [60], where the combination of copper foams and paraffin reached an effective conductivity as

high as 16 W·(m·K)$^{-1}$ with 4 pores per cm^2 and 88 % porosity, even though the thermal conductivity of paraffin is only ca. 0.2 W·(m·K)$^{-1}$.

Some key disadvantages of metallic foams include: reduced effective specific heat capacity in the energy storage container by displacement of PCM mass, and more importantly, high manufacturing cost in comparison with metallic fins.

4.1.2 Carbon inclusions

Beyond the effectiveness of metallic inclusions on the thermal response of PCM systems, the high thermal conductivity of some carbon-based materials makes them effective candidates for heat transfer enhancement. Two scales are to be considered for carbon-based materials: macroscale and nanoscale.

4.1.2.1 Macroscale carbon inclusions

Various types of macroscale carbon-based materials have been studied, including carbon fibers and graphite foams. Carbon fibers have been shown to be highly effective in increasing the effective thermal conductivity of PCMs [61, 62]. Thermo-physical properties of commercially available carbon fibers are typically as follows:

- Thermal conductivity: 50-220 W·(m·K)$^{-1}$
- Density: 2000-2260 kg·m^{-3}
- Specific heat capacity: ~500 J·(kg·K)$^{-1}$

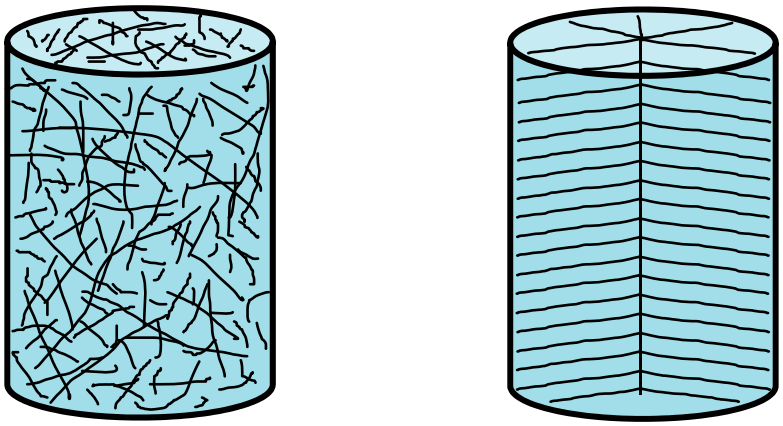

Figure 12: Randomly dispersed carbon fibers and "brush type" carbon fibers in a PCM container [3] (redrawn).

Carbon fibers are resistant to corrosion and are therefore appropriate for long term use. Their length can be as long as desired, though dimensions larger than the container will typically yield little or no higher thermal performance [62]. One study investigated two configurations for the carbon fibers into a cylindrical PCM container [62]: randomly dispersed in the container and a "brush type" design, as shown in Figure 12. The randomly dispersed configuration yielded 6 times higher thermal performance than without carbon fibers. With the brush type design, since the carbon fibers extended radially from the axis to the edge of the container and the outer shell of the cylinder was the heat sink, thermal performance was 3 times higher than with randomly dispersed configuration. The overall thermal performance was more enhanced by the higher effective conduction than it was negatively affected by the reduction in convective heat transfer.

Graphite foams are another popular choice as they feature high surface area to volume ratios. A typical encountered issue is the non-uniformity of the pore distribution of most graphite foams, leading to closed pores or higher difficulties to fill in the pores with PCM as compared to metallic foams [63-65]. Thermo-physical properties of graphite foam were found as follows:

- Thermal conductivity: 135-182 $W \cdot (m \cdot K)^{-1}$
- Density: 200-940 $kg \cdot m^{-3}$

Graphene aerogels have also been studied since they are the lightest known materials and exhibit a very high thermal conductivity, and therefore proved to yield high conductivity in PCM / graphene aerogel composites while displacing only the minimum of PCM mass [66]. While graphene aerogels start to be available commercially, their price remains very high, in the range of several hundreds USD per gram.

4.1.2.2 Nanoscale carbon inclusions

Another promising solution to enhance the heat conductivity through PCM mass is the inclusion of micro or nanoscale carbon-based materials within the PCM, since they feature exceptionally high intrinsic thermal conductivities and high surface area to volume ratios [3]. Exploiting the enhanced thermal properties of PCMs in play with nanoscale carbon materials requires a deeper understanding of the heat transfer processes. A detailed description of the thermal conductivity of nanoscale carbon materials has been given by Marconnet et al. [67].

4.1.3 Heat pipes

Heat pipes are designed to enhance the heat transfer between two bodies and rely on liquid-vapour phase change. At the hot surface, a liquid absorbs heat through conduction and turns into vapour. The vapour then travels along the heat pipe to the cold surface and condenses back into a liquid – releasing the latent heat. Through either capillary action, centrifugal force, or gravity, the liquid loops back to the hot surface to repeat the cycle.

The use of heat pipes to enhance heat transfer in a PCM system has gotten more attention in the recent years [68]. An experimental investigation of melting and solidification phenomena in a heat pipe-assisted PCM system reported that heat transfer between heat transfer fluid and PCM when using a heat pipe was twice higher than without heat pipe [69]. They also reported that using metallic fins alone as a heat transfer enhancement technique, did not yield significant improvement on the heat transfer. Instead, they recommended simultaneous use of heat pipe and fins.

Another study provided a three-dimensional simulation of a high temperature PCM system in the presence of radial finned heat pipes [70]. They reported that the heat pipe arrangement had a considerable effect on the acceleration of the charging process.

A recent and exhaustive state-of-the-art review on hybrid heat pipe latent heat storage systems [71] gathered findings from nearly 200 publications and is a recommended source of information on this topic.

4.2 PCM containment

PCM needs to be encapsulated so that the liquid phase cannot leak out of the containment. Such containment shall have the following properties [7], [72]:

- Meeting the technical requirements of strength, flexibility, corrosion resistance and thermal stability.
- Acting as a barrier to protect the PCM from harmful interaction with the environment.
- Sufficient surface for heat transfer.
- Structural stability and easy handling.

The classification of encapsulation methods is dependent mostly on the size of the single containment volume [7], [72], [3], i.e.:

- Bulk storage in tank heat exchangers with material of the tank shell dependent on the application (plastics, metal alloys, glass, ceramics). Requires an extensive heat transfer area between the PCM and heat transfer fluid in order to reach reasonably uniform temperature profile during PCM charging/discharging.
- Macroencapsulation: small containers of various shapes (rectangular prisms, tubes, spheres, elastic pouches) and size (down to 1 cm — 1 mm). Easy to manufacture, offer much more uniform temperature PCM profile than in the case of bulk storage; ullage (amount the container lacks to be full) may significantly degrade heat transfer for containers made of rigid construction materials,
- Microencapsulation: polymeric shell beads with diameter between 1 mm and 1 µm. Can be added to the heat transfer fluid, offering excellent PCM temperature profile. Microencapsulated PCMs have an excellent heat transfer performance because of the large area per volume of the capsules and the excellent cycling stability due to the restricted phase separation at microscopic distances [12]. When a microencapsulated PCM is dispersed in the heat transfer fluid, the resulting suspension forms a PCM slurry or emulsion.
- Nanoencapsulation: nanocoating of particles smaller than 1 µm. Extending all the advantages of microencapsulation.

Alternatively, PCM can be applied directly without any containment, either (1) as a PCM slurry, such that the PCM is the heat transfer fluid, increasing the thermal capacity and heat transfer rate; or (2) as a shape-stabilised PCM, where the whole PCM package constitutes a composite block of working phase-change-undergoing material and supporting structural material (the supporting material remains in solid phase even when the working material melts) [13]. A disadvantage for the first option is the high viscosity of slurries, while the second option yields lowered latent heat per composite volume.

The listed approaches for contained PCM are further detailed in the following sections; on a general level for micro-, nano-, macro- and bulk encapsulation and shape-stabilized PCMs, and thereafter specifically for low- and high-temperature applications.

4.2.1 Micro- and nanoencapsulation

The typical micro- and nanoencapsulation (often referred to as core-shell) PCMs are composed of core and shell layers, which can be classified as mononuclear, polynuclear or matrix type, as presented in Figure 12 [73].

Microencapsulation of PCM is created in a physical or chemical process in which tiny PCM particles or droplets are surrounded by a coating material, or embedded in a homogeneous or heterogeneous matrix. Physical methods encompass spray cooling, spray drying and fluidized bed processes while chemical methods involve various forms of polymerization (see Table 4).

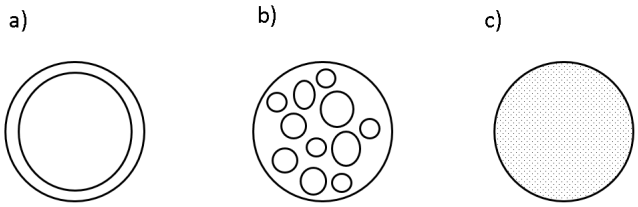

Figure 13: Structure of mononuclear a), polynuclear b), and matrix c) microencapsulated PCM or nanoencapsulated PCM.

Table 4: Classification of encapsulation methods for core-shell PCM structures [74].

Method			Organic PCM	Inorganic PCM
Chemical		Suspension polymerization	yes	no
		Dispersion	yes	no
		Emulsion	yes	yes
		In-situ polymerization	yes	yes
		Interfacial polymerization	yes	yes
		Electroplating	yes	yes
Physical	Physico-chemical	Coacervation	yes	no
		Sol-gel process	yes	yes
		Supercritical CO_2-assisted method	yes	no
	Physico-mechanical	Spray-drying	yes	no
		Electrostatic encapsulation	yes	no
		One-step method	yes	no
Mechanical packaging			yes	yes
Mechanical + electroplating			no	yes

4.2.2 Macro- and bulk encapsulation

Macro- and bulk encapsulation comprises the inclusion of PCM in various forms of tubes, pouches, spheres, panels or other receptacles [7]. Macro- and bulk encapsulation essentially solves the issue of containing the melted PCM in applications where the PCM is not already contained and should not leak to the heat transfer fluid. Through this containment, a number of possibilities have emerged to re-think the way the PCM could exchange heat with a given environment.

Regarding commercial solutions, PCM Products Ltd. (pcmproducts.net) provides, for example, the FlatICE^{TM} containers (see Figure 14), holding ca. 5 kg of PCM. The high-density polyethylene containers can be stacked together, thanks to internal support beams as well as external guides (see Figure 14), leaving clearance between the containers to allow a heat transfer fluid to circulate through. The method removes the need for dedicated heat exchangers in some cases, for example, by directly attaching the containers to a ceiling to passively regulate the room air temperature. Such solutions ease the deployment of LHTES solutions to a larger range of applications by removing the need of a complex heat exchanger design.

However, low-cost plastic-based containers often offer a limited range of temperature for applications due to softening of the plastic above 40-50 °C and thereafter lower material strength. Other encapsulation materials may be considered for higher temperature ranges (e.g. metal alloys, ceramic, advanced polymers) though the overall cost of encapsulation may be much higher.

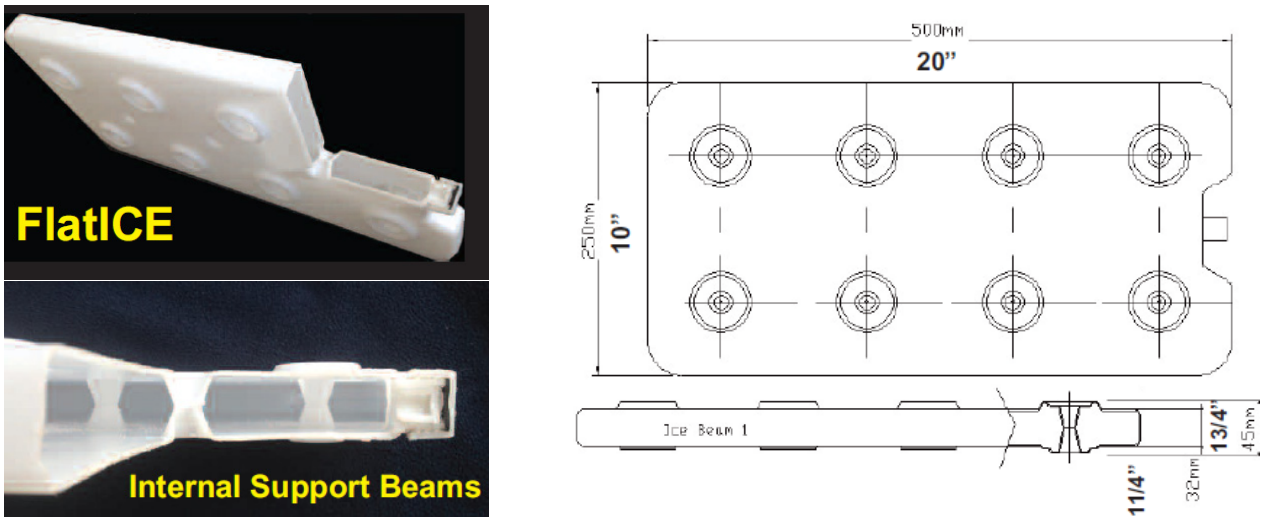

Figure 14: The FlatICE^{TM} container provided by PCM Products Ltd. (pcmproducts.net).

4.2.3 Shape-stabilized PCM

Direct integration of PCM with the supporting material means manufacturing a PCM identified as shape-stabilized, i.e., a PCM composite together with the other shape-maintaining material. Shape-stabilized PCMs allow phase change materials to retain the shape of the solid structure during the phase transition (avoiding phase segregation). Moreover, they provide suitable overall thermal conductivity and good compatibility with other construction materials. Six shape-stabilized PCM encapsulation techniques have been used so far: melt infiltration, cold compression, uniform mixing, vacuum impregnation, cold infiltration and sol-gel [74].

4.2.4 Low-temperature applications

Most commonly used forms of encapsulation in LT applications are spherical, prismatic or cylindrical capsules (nodules) made of plastic, glass, or metals, filling a storage tank through which a chilled glycol or other antifreeze heat transfer fluid is circulated at a low velocity [75], [76]. During the charge mode, the temperature of the heat transfer fluid is lower than the phase change temperature of the PCM, causing solidification of the encapsulated PCM. During discharging, the warm fluid carrying energy from the load absorbs the energy of the nodules, thus melting the PCM. A selection of commercially available microencapsulation products is presented in Table 5.

Most of the LHTES applications involving macroencapsulation are today dedicated to LT storage, due to the high availability and low cost of plastic materials to contain the PCM.

Table 5: Thermal properties of selected microencapsulated PCMs for low-temperature applications [12].

Core material	Melting temp. *(°C)*	Heat of fusion *(kJ·kg^{-1})*	Specific gravity	Capsule composition *(wt.%)*	Mean particle size *(μm)*	Final form
***n*-Decane**	-30	140-150	0.9	85-90 PCM 10-15 polymer shell	17-20	Wet filter cake or dry powder
***n*-Dodecane**	-9.5	150-160	0.9	85-90 PCM 10-15 polymer shell	17-20	Wet filter cake or dry powder

4.2.5 High-temperature applications

The potential shell materials for high-temperature encapsulation might be split into three groups depending on the type of material, i.e., metallic, inorganic and plastic (see Table 6). The majority of high-temperature macroencapsulations are fabricated using a metallic shell (see Table 7), while the high-temperature microencapsulations are mainly fabricated using plastic shells (see Table 8). The reason is ease of fabrication of metallic shells on macroscale and plastic shells on microscale.

Table 6: Potential shell materials for high-temperature applications [72].

Group	Potential materials	Advantages	Disadvantages	Potential applications
Metallic	Steel (stainless & carbon), nickel-chromium/carbon/ruthenium	High mechanical strength, can form an encapsulation using a variety of methods, high thermal stability at 1000 °C	High potential for corrosion, expensive	For high-temperature cases where ceramic shells are inappropriate e.g. liquid metal as the heat transfer fluid
Inorganic	Silicon dioxide, titanium dioxide, sodium silicate, calcium carbonate, silica	High thermal stability at 1000 °C, high mechanical strength, less expensive than metallic shells	Porous shell can lead to leakage	For certain high-temperature cases e.g. power generation, high-temperature industrial processes (cement and metal manufacturing)
Plastic	Melamine-formaldehyde, vinyltrimethoxysilane, urea-formaldehyde resin, polystyrene, poly(urethane-urea), styrene and methyl methacrylate, etc.	Can form an encapsulation using a variety of methods, less expensive than metallic shells	Relatively low thermal stability (max. 400 °C), low thermal conductivity	For cases with expected energy storage temperatures between 300 °C and 400 °C, e.g., building cooling, food and paper manufacturing

Table 7: Examples of metallic macroencapsulation materials for HT applications [72].

Shell material	Core material	Thermal stability temperature in the test *(°C)*	Theoretical melting point of the shell material *(°C)*
Steel	Paraffin wax	36	1370
Chromium-nickel	Copper	> 1150	-
Stainless steel 304L	Magnesium chloride	> 750	-
Stainless steel 304L/carbon steel 1018	Molten salt	> 470	-
Sodium silicate	Molten salt	300	1088
Carbon steel	Molten salt	800	1370
Silicon dioxide	Sodium nitrate	300-500	1600
Metallic-ceramic	Molten salt	300-800	-
Stainless steel	Paraffin wax	-	1400
Nickel	Lead	400	1445
Nickel	Copper	> 1100	-

Table 8: Examples of plastic microencapsulation materials for HT applications [72].

Shell material	Core material	Thermal stability temperature in the test *(°C)*	Theoretical melting point of the shell material *(°C)*
Titanium dioxide	Paraffin wax	240	1843
Sodium silicate	*n*-Octadecane	> 375	1088
Melamine–formaldehyde	Hexadecane	388	-
Vinyltrimethoxysilane	*n*-Octadecane	318.2	-
Urea-formaldehyde resin	Stearyl-alcohol	250-350	-
Calcium-carbonate	*n*-Octadecane	215	825
p(butyl methacrylate) + p(butyl acrylate)	*n*-Octadecane	380	-
Poly(methyl methacrylate-co-divinylbenzene) copolymer	Binary mixture of butyl stearate and paraffin	375-475	-
Poly(urea–urethane)	Xylitol	350	-
Silicon dioxide	Paraffin wax	292	1600
Styrene and methyl methacrylate	Paraffin wax	320-325	-
Silica	*n*-Octadecane	325	-
Melamine–formaldehyde	*n*-Dodecanol	371-404	-
Polystyrene	Paraffin wax	340	-

4.2.6 Thermo-physical characterization of encapsulated PCM

It is important that encapsulation does not deteriorate the thermo-physical properties (phase change temperature range, conductivity, latent heat of fusion and stability) of the PCM significantly. In practical applications, at least some of those properties might be degraded, as detailed below. On the other hand, encapsulation may reduce or even eliminate supercooling and phase segregation.

4.2.6.1 Phase change temperature range

The phase change temperature values of encapsulated PCMs present an irregular behaviour. Both increment and decrement of the melting temperature are possible, depending strongly on the type, thickness and diameter of the containment. Typically, the offset does not exceed 2-3 Kelvins [74].

4.2.6.2 Latent heat of fusion

Latent heat of fusion decreases for almost all core-shell encapsulated PCMs due to the decrease of core material mass fraction and strong interface interactions between core and shell. The decrement rate might be as high as 80 %. For shape-stabilized PCMs the latent heat of fusion of the resulting composite is directly proportional to the PCM weight fraction [74].

4.2.6.3 Thermal conductivity

The thermal conductivity of the shell may affect the resulting properties of encapsulated PCMs. If the thermal conductivity of the shell is lower than that of the PCM, the shell can hinder the heat transfer through the PCM, which also entails an increase in melting temperature. For shape-stabilized PCM composites, the conductivity might be greatly enhanced by employing high thermal conductivity stabilizing materials.

4.2.6.4 Degree of supercooling

Encapsulation with microcapsules plays a significant role in reducing supercooling for inorganic salt hydrates. It has been seen experimentally that encapsulation accelerates nucleation of hydrated salts for core-shell PCMs, most likely due to the relatively large specific surface area, promoting heterogeneous nucleation in shell wall cavities [74]. In cases where supercooling may constitute a significant challenge, a nucleating agent might be added to the core material to catalyse nucleation [77].

5 CFD modelling of PCM storage systems

Computational Fluid Dynamics (CFD) modelling of LHTES systems offers many advantages while designing PCM applications. For a given PCM system, one-dimensional calculations enable to obtain a rough estimate of the system performance. Beyond that, 2D and 3D modelling will enable system dimensioning and performance characterisation at a relatively low cost compared to direct testing in laboratory.

Once a system is properly modelled, dynamic modelling can be applied to simulate the behaviour of the modelled system with time-dependent boundary conditions and evaluate the system response. This is of special interest for the final selection of the PCM medium, fine dimensioning of the heat exchanger and fine-tuning the selected heat transfer enhancement method. Dynamic CFD simulations based on expected thermal cycles enable to evaluate the system efficiency, charging and discharging times and to ensure that the temperature is kept at all times under the degradation temperature in the whole PCM volume.

However, reliability of the CFD model is essential to achieve all the above-mentioned advantages. A few challenges arise in reality that may not be properly treated in the CFD models, such as supercooling or thermal degradation. Dynamic modelling shall also reflect properly the varying boundary conditions that the TES would experience in reality. Furthermore, experimental validation at an early stage of the modelling are often missing in the studies reported in the literature, leading to questionable results.

This section gives an overview of various typical CFD modelling challenges reported in the literature, as well as a few detailed examples of CFD simulations using ANSYS Fluent.

5.1 Modelling the solid/liquid boundary (Stefan problem)

Phase transition of a material is described by a particular kind of boundary value problems for partial differential equations, where phase boundary can move with time. This type of problems is often referred to as Stefan-problem, named after the Slovene physicist Jozef Stefan. The Stefan number, *Ste*, is the ratio of specific heat capacity to latent heat of fusion *ΔH* as given in the equation below:

$$Ste = \frac{c_p \Delta T}{\Delta H} \tag{9}$$

where *ΔT* is the difference in temperature between the heat source/sink and the melting temperature of the material, and c_p is the specific heat of the solid PCM. Most PCMs will have high latent heat with respect to the sensible heat capacity and hence a low Stefan number.

The classical assumptions made in order to solve a Stefan problem are that the situation is one-dimensional and semi-infinite, the PCM properties are constant, the heat source has constant temperature and the melt front is a distinct edge. This is illustrated in Figure 15.

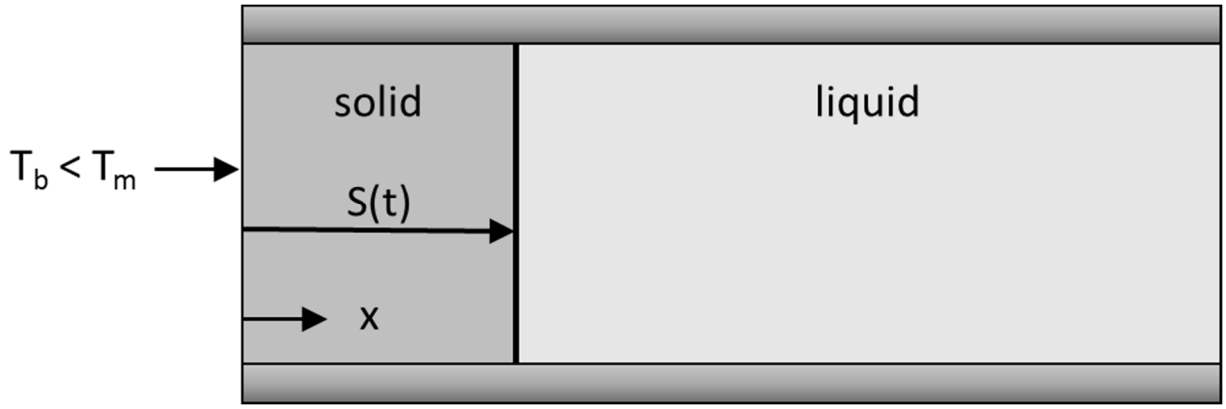

Figure 15: Classical Stefan problem formulation with solidification from left to right. T_b is the wall temperature on the left-side boundary, T_m is the PCM melting temperature, S(t) is the time-dependent position of the melt front.

However, this process can be quite complex in reality. The Stefan problem formulation ignores convection in the melting phase. If including natural convection, the motion of the melt front becomes two-dimensional which increases the modelling complexity.

The different classes of solutions available for the Stefan problem are analytical and numerical. The analytical methods are normally approximate, limited to one-dimensional analysis and they become very complicated when applied to multidimensional problems [4]. Numerical solutions may allow more precise description of the system dynamics, though, the higher the model complexity, the longer the computing time.

5.2 Modelling the heat transfer

The heat transfer phenomena in solid-liquid PCMs can be analysed using two main methods: temperature-based and enthalpy-based methods [78]. Using the first method, the energy conservation equations for the solid and the liquid phase are written separately with the temperature as the sole dependent variable. The solid-liquid interface can then be tracked explicitly to achieve an accurate solution for the problem [78].

In the enthalpy-based method, one energy conservation equation is used for the two phases, and the phase change problem becomes much simpler [4]. Advantages with this method are that (1) the governing equations are similar to the single-phase equations, (2) no explicit conditions need to be satisfied at the solid-liquid interface, and (3) the enthalpy formulation involves the solution within a mushy zone, involving both solid and liquid materials, between the two pure phases [78]. Using this method, the solid-liquid interface does not need to be tracked.

The mushy zone is a region in which the liquid fraction lies between 0 and 1, and hence a porosity can be defined which decreases from 1 to 0 as the material solidifies. When the material has fully solidified in a cell, the porosity becomes zero and hence the velocities also drop to zero. An appropriate momentum sink term is added to the momentum equation to account for the pressure drop caused by the presence of solid material. Similar sink terms are also added to all the turbulence equations to account for reduced porosity due to solid matter in the mushy and solidified regions [79].

Using $\vec{v}$ as the fluid velocity, the source term $\vec{S}$ in the momentum equation, as detailed by Al-Abidi et al. [80], is defined as:

$$\vec{S} = C(1-\beta)^2 \frac{\vec{v}}{\beta^3 + \varepsilon} \tag{10}$$

The source term, $\vec{S}$, follows the Darcy's law and is added to the momentum equation due to the phase change effect on convection, where $\frac{C(1-\beta)^2}{\beta^3+\varepsilon}$ is the ''porosity function" defined by Brent et al. [81] to make the momentum equations behave similarly to the Carmane-Kozeny equations for flow in porous media. The mushy zone constant, *C*, reflects the kinetic processes in the mushy zone morphology. It describes how steeply the velocity is reduced to zero when the material solidifies, this constant is varied between 10^4 and 10^7. Larger *C* values may lead to unphysical oscillations in the results. ε is a small computational constant (0.001) to prevent division by zero.

The liquid fraction, β, during the phase change between solid and liquid states when the temperature is $T_l \geq T \geq T_s$, can be expressed as follows:

$$\beta = \frac{\Delta H}{L} \tag{11}$$

$$\beta = \begin{cases} 0, & \text{if } T < T_s \\ 1, & if \ \ T > T_l \\ \frac{T - T_s}{T_l - T_s}, & \text{if } \ T_l \geq T \geq T_s \end{cases} \tag{12}$$

where *ΔH* is the latent heat content that may change between zero (solid) and the latent heat of fusion of the PCM (liquid).

5.3 Fixed mesh vs Adaptive mesh

The grid density at the melt front has to be quite high in order to reasonably describe the physical processes that occur in this area. One could use a uniform grid having a spacing fine enough so that the local errors estimated in these difficult regions are acceptable, though, computationally-speaking, this approach is extremely costly. As this high density is not needed in other parts of the domain, it is natural to adapt the grid density to the local physical conditions to improve the computational efficiency.

The melt front will move during the simulation, and there are two main approaches for solution-based grid adaption to handle this: a local mesh refinement method and a moving mesh method. The former model starts with a uniform grid, and at each iteration grid points are added or removed to satisfy the required accuracy. The main challenge with this method is connected to the data structures as the number of grid points and the distribution are changing between each time step. The moving mesh method starts with a uniform mesh and moves the grid points during the simulation, keeping the number of grid points and the topology fixed [82].

In general, time variant mesh adaption gives good accuracy, but it is limited to quite simple problems and geometries. The fixed mesh approach is simpler to use for more complicated, practical applications [4]. This approach is sufficient to be used in combination with the enthalpy based heat transfer method.

5.4 Examples of CFD simulations using ANSYS Fluent

While other CFD codes can also be used for modelling PCM systems, such as Comsol or OpenFoam for instance, the following section focuses on applications using ANSYS Fluent since it is the software that will be used in the current project.

ANSYS Fluent software is a commercially available, general-purpose CFD code, based on finite volume element calculation method, and which has been widely used for modelling PCM systems. ANSYS Fluent allows for phase change simulations of PCM through the enthalpy porosity method. This means that instead of tracking the liquid-solid front explicitly, the liquid-solid mushy zone (partially solidified region) is treated as a porous zone. The porosity in each cell is set equal to the liquid fraction in that cell, which indicates the fraction of the cell volume that is in liquid form. The liquid fraction is computed at each iteration, based on an enthalpy balance [79].

ANSYS Fluent also allows for modelling of thermal and solutal buoyancy, which is often important for accurate prediction of the overall solidification behaviour. Thermal buoyancy is the gravitational force due to the variation of density with temperature, and causes a flow that tends to promote mixing, and smooths out temperature gradients. The phenomenon is also known as natural convection. Solutal buoyancy is the gravitational force due to the variation of density with the change in the species composition of the melt, which moves the enriched liquid away from the liquid-solid interface and replaces it with the far field nominal composition [79].

Dutil et al. [82] have reviewed the scientific literature on numerical models of PCM used in thermal storage applications, with classification by their geometrical configuration (rectangular, spherical and cylindrical geometry, packed beds, finned geometry, porous and fibrous materials, and slurry) and then by application. Al-Abidi [78] claims that even if other CFD software can be used to simulate the PCM process, ANSYS Fluent is often preferred by most researchers for this type of problems. They give a review of successful simulations of the application of PCM in different engineering applications, with emphasis on simulations performed with ANSYS Fluent. Some examples relevant for the current work are summarized in the following sections.

5.4.1 Cylindrical geometries

Shmueli et al. [83] investigated melting of a PCM in a vertical cylindrical tube numerically and validated the results against experimental data. The investigated tube diameters were 3 and 4 cm, the tube was exposed to air at the top, insulated at the bottom and the wall temperature was between 10 and 30 °C above the melting temperature of the PCM (see Figure 16). The PCM properties were based on the commercially available material RT27 with a melting interval of 26-28 °C.

ANSYS Fluent 6.2 solver was used for the simulations, and the enthalpy–porosity approach was adopted for the PCM. Natural convection was included for the PCM. Both three- and two-dimensional (axisymmetric) models were explored, and no considerable difference was found between them. The total number of cells was 13,652 (2D). The time step in the calculations was as small as 0.002 s, with the convergence criterion of 10^{-3} for the velocity components and continuity, and criterion of 10^{-6} for energy. At the time of the reporting, in 2010, the authors reported that typical computing time of a complete melting would take from three weeks to two months, depending on the tube diameter and applied temperature difference. Computing time has however significantly improved in the last decade. Unless supercomputers are used, simulating phase changes in a PCM system remains time-consuming, though the computing time is rather in the range of several hours to several days for a sufficiently fine grid.

Shmueli et al. then analysed the influence of the term describing the mushy zone in the momentum equation to the melting process, and concluded that there should exist an optimum value of the mushy zone constant *C* included in this term. The higher the *C* value, the longer the melting time. However, above $C = 10^8$, the results were either similar to the results using values between 10^5 and 10^8 or not physical. It appears that within the range 10^5 and 10^8, there exists an optimal value for which the agreement with the corresponding experimental data would improve.

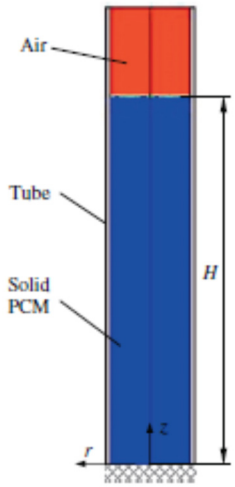

Figure 16: Shmueli's simulation model at t = 0 [83].

Almsater et al. [84] presented a CFD model using ANSYS Fluent 15.0 for PCM in a vertical triplex tube thermal energy storage system (TTTESS) and its validation through experimental results. It was found that the model accurately predicts the behaviour of the TTTESS during the melting and solidification processes. The outer and inner tube were used for the heat transfer fluid and the middle tube was used for the PCM. Eight fins were included to separate the PCM compartments (see Figure 17). Water was used as PCM, while Dynalen HC-50 was selected as the heat transfer fluid. Simulations results of the temperature at the heat transfer fluid's inlet and outlet, as well as at six locations in the PCM were compared with experimental results and showed good agreement. The model was able to predict the average PCM behaviour, as well as the duration of the phase change process at each experimental point.

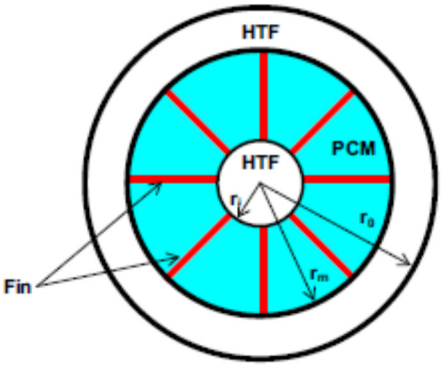

Figure 17: The physical configuration of the TTTESS by Almsater et al. [84].

The simulations were run as 3D, and the modelling of the phase change was based on the enthalpy-porosity formulation. Natural convection in the PCM was included. Three fixed grid resolutions (1.14, 2.15

and 4.65 million cells) were used, all predicting a phase change time of 161 minutes, and all with computing time of more than 12 days (the study was published in 2017).

Guo and Zhang [85] have proposed a new type of HT LHTES system structure using aluminium foils to improve the heat transfer, which can be integrated into solar power generation using direct steam generation. The eutectic system KNO_3–$NaNO_3$ was selected as the PCM with a solidification temperature of 220 °C.

Their system was a typical foil-tube arrangement (see Figure 18). The aluminium foils were arranged orthogonally to the axis of the steam tubes. The PCM was initially liquid and filled the space around the tube, foil and shell, while the heat transfer fluid (water/steam) flowed inside the tube. The HT LHTES system had a cylindrical symmetry, and the computations could be reduced to two dimensions.

The study focused on the enhancement of the discharging process, and transient two-dimensional heat conduction problems were solved using ANSYS Fluent 6.2 using the enthalpy-porosity approach implemented in the software. Natural convection was assumed to have a negligible effect compared to the effect of heat conduction in the solidification process. Constant thermo-physical properties of the PCM were considered. The grid size was 60 (radial) x (15 (PCM axial) + 2 (foil thickness)), and the time step was set to 0.1 s. The computational results showed that adding aluminium foils was an efficient way to enhance the heat transfer in the HT LHTES, and illustrated how the heat transfer and discharge time are affected by the changes in geometry of the aluminium foil, tube radius (6 – 50 mm), boundary conditions and thermal conductivity of the PCM.

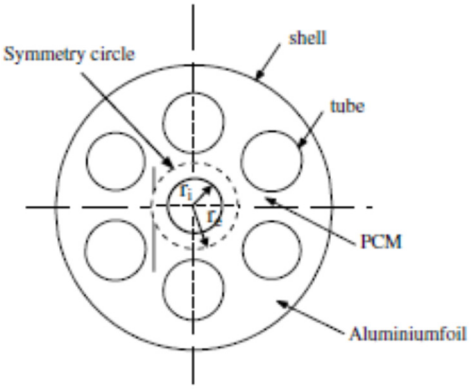

Figure 18 Schematic of the HT LHTES with aluminium foil in the study by Guo and Zhang [85].

5.4.2 Open multideck refrigerated display cabinet (MDC)

As mentioned in Section 3.1.3, Alzuwaid et al. [26] developed a 2D CFD model for a prototype refrigerated open type multideck display cabinet, with and without integrated PCM. Extensive experiments were conducted to validate the CFD model. The cabinet dimensions were 1.25 m x 0.85 m x 1.98 m (width x depth x height), 3.15 m^2 refrigerated area and 1.5 m display opening height. The cabinet was equipped with a single air curtain situated from the top (Figure 19).

Low-temperature airflow from the cabinet evaporator outlet, cooling the test food products, passed partly vertically in the back-flow channel of the cabinet and partly horizontally through the perforated back panel, before reaching the air curtain, as shown in Figure 19 (a). The cabinet utilized off-cycle for defrost and the allowed product temperature variation was from 0 to +4 °C. The intervals between defrost was 4 h, and

apart from the defrost periods the compressor also entered normal (smaller) cycles where on and off was controlled based on the thermostat temperature. The experiment period was 24 h.

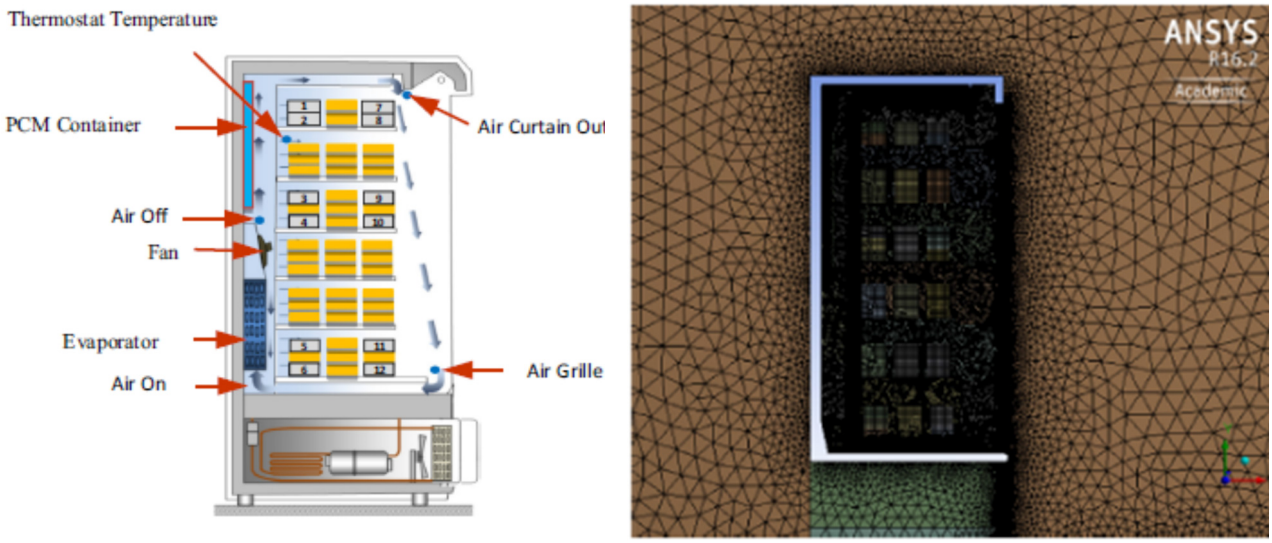

Figure 19: (Left) Side view of the Alzuwaid cabinet with products; (Right) Computational grid for the 2D CFD-model [26].

The 2D CFD model was developed using ANSYS Fluent 14. The solution-adaptive mesh refinement feature in ANSYS Fluent was used for mesh adaption resulting in a mesh size of 121 367 elements. The standard k-ε-turbulence model was applied, and the discrete ordinates method was used to simulate the coupling of radiative and convective heat transfer. The modelling of the solidification/melting process relied on the enthalpy-porosity technique.

The authors selected water as the PCM, and the PCM storage was modelled as a rectangular container unit installed on the back-panel flow duct wall of the cabinet just after the evaporator coils. The heat transfer to and from the PCM involved convection.

Three user-defined functions (UDFs) were included for the transient operation of the cabinet to (1) specify a heat source/sink in the evaporator region, (2) check the cabinet temperature at the thermostat sensor point at the end of each time step working as a thermostatic controller and (3) set initial values for flow quantities.

The authors reported that due to the complexity of the developed CFD model, several days of computing time were necessary for the transient simulations to approach stability. The study was published in 2016. The time step was set to 0.25 s, with maximum 20 iterations per time step.

The simulation results showed that significant energy savings can be obtained through the installation of a PCM container, and the authors reported that the validated model could be used to explore and analyse the cabinet performance and control strategies at various operating and design conditions.

6 Conclusions and recommendations for the PCM-Eff project

Throughout the review of the existing literature on thermal energy storage based on phase change materials, this research field appeared to have been extensively studied for more than a decade. Latent heat thermal energy storage (LHTES) solutions have already penetrated the thermal energy storage market through a handful of applications and upcoming innovative PCM-based solutions close to commercialisation are numerous and promising.

A number of applications where energy efficiency can be improved by utilizing LHTES have been presented in this report. Applications related to LT applications in refrigerated cabinets and medium- to high-temperature applications in small-scale wood stoves are of particular interest since being a focus of the PCM-Eff project. The report also focuses on the CFD modelling techniques to simulate effectively LHTES systems. A few key findings and recommendations are listed below:

- Beyond the logical focus on melting temperature, selecting the optimal PCM implies a deeper look at thermo-physical and chemical properties, nucleation and crystal growth and economics and usability. Systematic methods exist to ease the selection process and rank the PCM candidates.
- Degradation of the PCM over time is an essential risk to consider since the PCM properties might radically change as they degrade cycle after cycle. Thermal degradation is another key risk to consider. A rule of thumb says that the PCM temperature shall not be elevated more than 20-40 °C above the melting temperature. However, one should consider experimentally testing a PCM before using it or at least study the literature for a specific PCM before selecting it.
- Supercooling (and overheating) will not necessarily appear through modelling. Early validation experiments are generally required to evaluate the importance of such issues for a specific application. Various solutions exist to enhance nucleation or help dissipate high local temperature. This issue is especially important for LT applications where the temperature range is usually narrow.
- One main drawback of most PCMs, apart from metallic PCMs, is their low thermal conductivity. Hence, to obtain sufficient heat transfer between the PCM and the heat transfer fluid, as well as within the PCM, heat transfer enhancement methods should be employed. While there exist many methods, not all will fit the requirements of a specific application and various options shall be considered to find the best match. Cost and final heat capacity of the system shall not be forgotten in the evaluation.
- PCM encapsulation methods are especially relevant for applications where the nature of the PCM might be incompatible with its environment (e.g. PCM toxicity versus food storage). For LT applications, many commercial solutions are affordable and enable simplified LHTES design.
- Coupling wood stoves with LHTES has been explored but still lacks commercial applications. One main challenge pointed out, beyond the technical ones specified above, is the final product design. Aesthetics might be valued as much or more than performance by customers and should be thoroughly addressed from the early design phase to be able to take a solution to commercialization.
- In the case of CFD modelling with ANSYS Fluent, the agreement between computational data and experimental data for the PCM melting process seems to be sensitive to the mushy zone constant, *C,* used in the source term of the momentum equation to represent the influence of convection in the porosity zone. Therefore, fine tuning of *C* values should be performed when validating numerical models.

7 References

[1] A. Gil, M. Medrano, I. Martorell, A. Lázaro, P. Dolado, B. Zalba, L.F. Cabeza, State of the art on high temperature thermal energy storage for power generation. Part 1—Concepts, materials and modellization, Renewable and Sustainable Energy Reviews, 14 (2010) 31-55.

[2] A. Hoshi, D.R. Mills, A. Bittar, T.S. Saitoh, Screening of high melting point phase change materials (PCM) in solar thermal concentrating technology based on CLFR, Solar Energy, 79 (2005) 332-339.

[3] A.S. Fleischer, Thermal energy storage using phase change materials: fundamentals and applications, Springer, 2015.

[4] A. Sharma, V.V. Tyagi, C.R. Chen, D. Buddhi, Review on thermal energy storage with phase change materials and applications, Renewable and Sustainable Energy Reviews, 13 (2009) 318-345.

[5] A.F. Regin, S. Solanki, J. Saini, Heat transfer characteristics of thermal energy storage system using PCM capsules: a review, Renewable and Sustainable Energy Reviews, 12 (2008) 2438-2458.

[6] G. Hed, R. Bellander, Mathematical modelling of PCM air heat exchanger, Energy and Buildings, 38 (2006) 82-89.

[7] E. Oró, A. de Gracia, A. Castell, M.M. Farid, L.F. Cabeza, Review on phase change materials (PCMs) for cold thermal energy storage applications, Applied Energy, 99 (2012) 513-533.

[8] W.R. Sutterlin, Phase Change Materials, A Brief Comparison of Ice Packs, Salts, Paraffins, and Vegetable-derived Phase Change Materials, in: Pharmaceutical Outsourcing, 2011.

[9] ZAE Bayern - Materialklassen, die als PCM untersucht und eingesetzt werden, http://forschung-energiespeicher.info/waerme-speichern/projektliste/quickinfo-einzelansicht/Latentwaermespeicher-1/kapitel/2/, Accessed June 2017.

[10] K. Kristjansson, E. Næss, Ø. Skreiberg, Dampening of wood batch combustion heat release using a phase change material heat storage: Material selection and heat storage property optimization, Energy, 115, Part 1 (2016) 378-385.

[11] A.A. Al-Abidi, S. Bin Mat, K. Sopian, M.Y. Sulaiman, C.H. Lim, A. Th, Review of thermal energy storage for air conditioning systems, Renewable and Sustainable Energy Reviews, 16 (2012) 5802-5819.

[12] G. Li, Y. Hwang, R. Radermacher, H.-H. Chun, Review of cold storage materials for subzero applications, Energy, 51 (2013) 1-17.

[13] C. Veerakumar, A. Sreekumar, Phase change material based cold thermal energy storage: Materials, techniques and applications – A review, International Journal of Refrigeration, 67 (2016) 271-289.

[14] M. Mastani Joybari, F. Haghighat, J. Moffat, P. Sra, Heat and cold storage using phase change materials in domestic refrigeration systems: The state-of-the-art review, Energy and Buildings, 106 (2015) 111-124.

[15] F. Alzuwaid, Y.T. Ge, S.A. Tassou, A. Raeisi, L. Gowreesunker, The novel use of phase change materials in a refrigerated display cabinet: An experimental investigation, Applied Thermal Engineering, 75 (2015) 770-778.

[16] Teappcm - PCM Phase Change Material Materials Manufacturers, http://www.teappcm.com/, Accessed April 2017.

[17] Cristopia - The STL technology, https://www.cristopia.com/EN/la-technologie-stl.html, Accessed April 2017.

[18] Microtek Leads the Way in Encapsulation Technologies, http://www.microteklabs.com/, Accessed April 2017.

[19] Rubitherm GmbH. - Products, https://www.rubitherm.eu/en/productCategories.html, Accessed April 2017.

[20] Climator - Product data sheets, http://climator.com/product-data-sheets/?lang=en, Accessed April 2017.

[21] W. Lu, S.A. Tassou, Characterization and experimental investigation of phase change materials for chilled food refrigerated cabinet applications, Applied Energy, 112 (2013) 1376-1382.

[22] D.R. Cordray, L.R. Kaplan, P.M. Woyciesjes, T.F. Kozak, Solid - liquid phase diagram for ethylene glycol + water, Fluid Phase Equilibria, 117 (1996) 146-152.

[23] M. De Falco, M. Capocelli, A. Giannattasio, Performance analysis of an innovative PCM-based device for cold storage in the civil air conditioning, Energy and Buildings, 122 (2016) 1-10.

[24] V. Antony Aroul Raj, R. Velraj, Heat transfer and pressure drop studies on a PCM-heat exchanger module for free cooling applications, International Journal of Thermal Sciences, 50 (2011) 1573-1582.

[25] Y.L. Lu, W.H. Zhang, P. Yuan, M.D. Xue, Z.G. Qu, W.Q. Tao, Experimental study of heat transfer intensification by using a novel combined shelf in food refrigerated display cabinets (Experimental study of a novel cabinets), Applied Thermal Engineering, 30 (2010) 85-91.

[26] F.A. Alzuwaid, Y.T. Ge, S.A. Tassou, J. Sun, The novel use of phase change materials in an open type refrigerated display cabinet: A theoretical investigation, Applied Energy, 180 (2016) 76-85.

[27] B. Zalba, J.M. Marín, L.F. Cabeza, H. Mehling, Review on thermal energy storage with phase change: materials, heat transfer analysis and applications, Applied Thermal Engineering, 23 (2003) 251-283.

[28] T. Nomura, N. Okinaka, T. Akiyama, Technology of Latent Heat Storage for High Temperature Application: A Review, ISIJ International, 50 (2010) 1229-1239.

[29] M. Liu, W. Saman, F. Bruno, Review on storage materials and thermal performance enhancement techniques for high temperature phase change thermal storage systems, Renewable and Sustainable Energy Reviews, 16 (2012) 2118-2132.

[30] M.M. Kenisarin, High-temperature phase change materials for thermal energy storage, Renewable and Sustainable Energy Reviews, 14 (2010) 955-970.

[31] C. Mandl, I. Obernberger, Guidelines for heat storage units based on Phase Change Materials (PCM), in: E.-N. Bioenergy (Ed.) Project "Woodstoves2020", 2017.

[32] U. Zielke, M. Bjerrum, T. Nørgaard, Slow Heat Release - Brændeovn med salthydratvarmelager - Miljøprojekt nr. 1438, in: T. Institut (Ed.), 2013.

[33] M.S. Haugen, Termisk lagringssystem for vedovner, in: Institutt for energi og prosessteknikk, NTNU, 2012, pp. 92.

[34] F. Agyenim, N. Hewitt, P. Eames, M. Smyth, A review of materials, heat transfer and phase change problem formulation for latent heat thermal energy storage systems (LHTESS), Renewable and Sustainable Energy Reviews, 14 (2010) 615-628.

[35] J. Pereira da Cunha, P. Eames, Thermal energy storage for low and medium temperature applications using phase change materials – A review, Applied Energy, 177 (2016) 227-238.

[36] J.C. Gomez, High-Temperature Phase Change Materials (PCM) Candidates for Thermal Energy Storage (TES) Applications in, NREL, 2011.

[37] A. Fopah Lele, F. Kuznik, H.U. Rammelberg, T. Schmidt, W.K.L. Ruck, Thermal decomposition kinetic of salt hydrates for heat storage systems, Applied Energy, 154 (2015) 447-458.

[38] G. Setoh, F.L. Tan, S.C. Fok, Experimental studies on the use of a phase change material for cooling mobile phones, International Communications in Heat and Mass Transfer, 37 (2010) 1403-1410.

[39] Y. Tomizawa, K. Sasaki, A. Kuroda, R. Takeda, Y. Kaito, Experimental and numerical study on phase change material (PCM) for thermal management of mobile devices, Applied Thermal Engineering, 98 (2016) 320-329.

[40] R. Baetens, B.P. Jelle, A. Gustavsen, Phase change materials for building applications: A state-of-the-art review, Energy and Buildings, 42 (2010) 1361-1368.

[41] A. de Gracia, L.F. Cabeza, Phase change materials and thermal energy storage for buildings, Energy and Buildings, 103 (2015) 414-419.

[42] M. Kenisarin, K. Mahkamov, Passive thermal control in residential buildings using phase change materials, Renewable and Sustainable Energy Reviews, 55 (2016) 371-398.

[43] Á.Á. Pardiñas, M.J. Alonso, R. Diz, K.H. Kvalsvik, J. Fernández-Seara, State-of-the-art for the use of phase-change materials in tanks coupled with heat pumps, Energy and Buildings, 140 (2017) 28-41.

[44] A.A. Al-Abidi, S. Mat, K. Sopian, M.Y. Sulaiman, A.T. Mohammad, Numerical study of PCM solidification in a triplex tube heat exchanger with internal and external fins, International Journal of Heat and Mass Transfer, 61 (2013) 684-695.

[45] Rubitherm - Phase Change Materials, https://www.rubitherm.eu/en/, Accessed April 2017.

[46] B. Xu, P. Li, C. Chan, Application of phase change materials for thermal energy storage in concentrated solar thermal power plants: A review to recent developments, Applied Energy, 160 (2015) 286-307.

[47] S. Kuravi, J. Trahan, D.Y. Goswami, M.M. Rahman, E.K. Stefanakos, Thermal energy storage technologies

and systems for concentrating solar power plants, Progress in Energy and Combustion Science, 39 (2013) 285-319.

[48] L. Miró, J. Gasia, L.F. Cabeza, Thermal energy storage (TES) for industrial waste heat (IWH) recovery: A review, Applied Energy, 179 (2016) 284-301.

[49] T. Steinparzer, M. Haider, A. Fleischanderl, A. Hampel, G. Enickl, F. Zauner, Heat exchangers and thermal energy storage concepts for the off-gas heat of steelmaking devices, Journal of Physics: Conference Series, 395 (2012) 012158.

[50] N.R. Jankowski, F.P. McCluskey, A review of phase change materials for vehicle component thermal buffering, Applied Energy, 113 (2014) 1525-1561.

[51] R.W. Johnson, J.L. Evans, P. Jacobsen, J.R. Thompson, M. Christopher, The changing automotive environment: high-temperature electronics, IEEE Transactions on Electronics Packaging Manufacturing, 27 (2004) 164-176.

[52] C. Benesch, M. Blank, R. Scharler, M. Kössl, I. Obernberger, Transient CFD Simulation of Wood Log Stoves with Heat Storage Devices, in: 21st European Biomass Conference and Exhibition, 2015, pp. 578-584.

[53] I. Obernberger, C. Mandl, M. Kössl, Improved low emission and high efficiency wood stove with integrated PCM heat exchanger, in: European Biomass Conference and Exhibition - EUBCE 2017 - Workshop "Wood Stoves 2020", 2017.

[54] V. Shatikian, G. Ziskind, R. Letan, Numerical investigation of a PCM-based heat sink with internal fins: Constant heat flux, International Journal of Heat and Mass Transfer, 51 (2008) 1488-1493.

[55] S.K. Saha, P. Dutta, Heat transfer correlations for PCM-based heat sinks with plate fins, Applied Thermal Engineering, 30 (2010) 2485-2491.

[56] P.P. Levin, A. Shitzer, G. Hetsroni, Numerical optimization of a PCM-based heat sink with internal fins, International Journal of Heat and Mass Transfer, 61 (2013) 638-645.

[57] S.F. Hosseinizadeh, F.L. Tan, S.M. Moosania, Experimental and numerical studies on performance of PCM-based heat sink with different configurations of internal fins, Applied Thermal Engineering, 31 (2011) 3827-3838.

[58] K. Chintakrinda, R.D. Weinstein, A.S. Fleischer, A direct comparison of three different material enhancement methods on the transient thermal response of paraffin phase change material exposed to high heat fluxes, International Journal of Thermal Sciences, 50 (2011) 1639-1647.

[59] C.Y. Zhao, W. Lu, Y. Tian, Heat transfer enhancement for thermal energy storage using metal foams embedded within phase change materials (PCMs), Solar Energy, 84 (2010) 1402-1412.

[60] X. Xiao, P. Zhang, M. Li, Effective thermal conductivity of open-cell metal foams impregnated with pure paraffin for latent heat storage, International Journal of Thermal Sciences, 81 (2014) 94-105.

[61] F. Samimi, A. Babapoor, M. Azizi, G. Karimi, Thermal management analysis of a Li-ion battery cell using phase change material loaded with carbon fibers, Energy, 96 (2016) 355-371.

[62] J. Fukai, M. Kanou, Y. Kodama, O. Miyatake, Thermal conductivity enhancement of energy storage media using carbon fibers, Energy Conversion and Management, 41 (2000) 1543-1556.

[63] J.-l. Song, Q.-g. Guo, Y.-j. Zhong, X.-q. Gao, Z.-h. Feng, Z. Fan, J.-l. Shi, L. Liu, Thermophysical properties of high-density graphite foams and their paraffin composites, New Carbon Materials, 27 (2012) 27-34.

[64] R. Warzoha, O. Sanusi, B. McManus, A.S. Fleischer, Development of Methods to Fully Saturate Carbon Foam With Paraffin Wax Phase Change Material for Energy Storage, Journal of Solar Energy Engineering, 135 (2012) 021006-021006-021008.

[65] Y. Zhong, Q. Guo, S. Li, J. Shi, L. Liu, Heat transfer enhancement of paraffin wax using graphite foam for thermal energy storage, Solar Energy Materials and Solar Cells, 94 (2010) 1011-1014.

[66] Y. Zhong, M. Zhou, F. Huang, T. Lin, D. Wan, Effect of graphene aerogel on thermal behavior of phase change materials for thermal management, Solar Energy Materials and Solar Cells, 113 (2013) 195-200.

[67] A.M. Marconnet, M.A. Panzer, K.E. Goodson, Thermal conduction phenomena in carbon nanotubes and related nanostructured materials, Reviews of Modern Physics, 85 (2013) 1295-1326.

[68] R. Yogev, A. Kribus, PCM Storage System with Integrated Active Heat Pipe, Energy Procedia, 49 (2014) 1061-1070.

[69] C.W. Robak, T.L. Bergman, A. Faghri, Enhancement of latent heat energy storage using embedded heat pipes, International Journal of Heat and Mass Transfer, 54 (2011) 3476-3484.

[70] S. Tiari, S. Qiu, Three-dimensional simulation of high temperature latent heat thermal energy storage system assisted by finned heat pipes, Energy Conversion and Management, 105 (2015) 260-271.

[71] M.S. Naghavi, K.S. Ong, M. Mehrali, I.A. Badruddin, H.S.C. Metselaar, A state-of-the-art review on hybrid heat pipe latent heat storage systems, Energy Conversion and Management, 105 (2015) 1178-1204.

[72] R. Jacob, F. Bruno, Review on shell materials used in the encapsulation of phase change materials for high temperature thermal energy storage, Renewable and Sustainable Energy Reviews, 48 (2015) 79-87.

[73] W. Su, J. Darkwa, G. Kokogiannakis, Review of solid–liquid phase change materials and their encapsulation technologies, Renewable and Sustainable Energy Reviews, 48 (2015) 373-391.

[74] Y.E. Milián, A. Gutiérrez, M. Grágeda, S. Ushak, A review on encapsulation techniques for inorganic phase change materials and the influence on their thermophysical properties, Renewable and Sustainable Energy Reviews, 73 (2017) 983-999.

[75] J.P. Bédécarrats, J. Castaing-Lasvignottes, F. Strub, J.P. Dumas, Study of a phase change energy storage using spherical capsules. Part I: Experimental results, Energy Conversion and Management, 50 (2009) 2527-2536.

[76] S.-L. Chen, C.-L. Chen, C.-C. Tin, T.-S. Lee, M.-C. Ke, An experimental investigation of cold storage in an encapsulated thermal storage tank, Experimental Thermal and Fluid Science, 23 (2000) 133-144.

[77] G. Li, Y. Hwang, R. Radermacher, Review of cold storage materials for air conditioning application, International Journal of Refrigeration, 35 (2012) 2053-2077.

[78] A.A. Al-Abidi, S. Bin Mat, K. Sopian, M.Y. Sulaiman, A.T. Mohammed, CFD applications for latent heat thermal energy storage: a review, Renewable and Sustainable Energy Reviews, 20 (2013) 353-363.

[79] ANSYS, Fluent Theory Guide, Release 16.1, 2015.

[80] A.A. Al-Abidi, S. Mat, K. Sopian, M.Y. Sulaiman, A.T. Mohammad, Internal and external fin heat transfer enhancement technique for latent heat thermal energy storage in triplex tube heat exchangers, Applied Thermal Engineering, 53 (2013) 147-156.

[81] A.D. Brent, V.R. Voller, K.J. Reid, Enthalpy-porosity technique for modeling convection-diffusion phase change: Application to the melting of a pure metal, Numerical Heat Transfer, 13 (1988) 297-318.

[82] Y. Dutil, D.R. Rousse, N.B. Salah, S. Lassue, L. Zalewski, A review on phase-change materials: Mathematical modeling and simulations, Renewable and Sustainable Energy Reviews, 15 (2011) 112-130.

[83] H. Shmueli, G. Ziskind, R. Letan, Melting in a vertical cylindrical tube: Numerical investigation and comparison with experiments, International Journal of Heat and Mass Transfer, 53 (2010) 4082-4091.

[84] S. Almsater, A. Alemu, W. Saman, F. Bruno, Development and experimental validation of a CFD model for PCM in a vertical triplex tube heat exchanger, Applied Thermal Engineering, 116 (2017) 344-354.

[85] C. Guo, W. Zhang, Numerical simulation and parametric study on new type of high temperature latent heat thermal energy storage system, Energy Conversion and Management, 49 (2008) 919-927.

[86] Thermal Energy Storage - Technology Brief, in: IEA-ETSAP and IRENA Technology Brief E17 – January 2013.

[87] E. A.R., Techno-Economic Assessment of Thermal Energy Storage Integration into Low Temperature District Heating Networks, in, KTH School of Industrial Engineering and Management, 2016.

[88] M. Lanahan, P. Tabares-Velasco, Seasonal Thermal-Energy Storage: A Critical Review on BTES Systems, Modeling, and System Design for Higher System Efficiency, Energies, 10 (2017) 743.

[89] D. Fernandes, F. Pitié, G. Cáceres, J. Baeyens, Thermal energy storage: "How previous findings determine current research priorities", Energy, 39 (2012) 246-257.

[90] Energy Nest AS, www.energy-nest.com, Accessed June 2017.

[91] C. Greiner, Høy-temperatur termisk energilager - Energy Nest AS, in: Bellona Seminar energilagring, 2016.

[92] M. Montané, G. Cáceres, M. Villena, R. O'Ryan, Techno-Economic Forecasts of Lithium Nitrates for Thermal Storage Systems, Sustainability (2071-1050), 9 (2017) 1-15.

[93] G. Brundrett, Harnessing renewable energy in electric power systems – theory, practice, policy, edited by Boaz Moselle, Jorge Padilla, Richard Schmalensee, International Journal of Ambient Energy, 32 (2011) 57-58.

[94] D. Kearney, U. Herrmann, P. Nava, B. Kelly, R. Mahoney, J. Pacheco, R. Cable, N. Potrovitza, D. Blake, H. Price, Assessment of a Molten Salt Heat Transfer Fluid

in a Parabolic Trough Solar Field, Journal of Solar Energy Engineering, 125 (2003) 170-176.

[95] Norsk Kleber AS, www.norskkleber.no, Accessed June 2017.

[96] E. John, M. Hale, P. Selvam, Concrete as a thermal energy storage medium for thermocline solar energy storage systems, Solar Energy, 96 (2013) 194-204.

[97] B. R.K., IEA ECES IA Case studies - Brief Country Report Norway, in, Norwegian Geotechnical Institute, 2013.

[98] L. Gao, J. Zhao, Z. Tang, A Review on Borehole Seasonal Solar Thermal Energy Storage, Energy Procedia, 70 (2015) 209-218.

[99] Rock Energy AS, www.rockenergy.no, Accessed June 2017.

[100] L.F. Cabeza, E. Galindo, C. Prieto, C. Barreneche, A. Inés Fernández, Key performance indicators in thermal energy storage: Survey and assessment, Renewable Energy, 83 (2015) 820-827.

[101] H. Chen, T.N. Cong, W. Yang, C. Tan, Y. Li, Y. Ding, Progress in electrical energy storage system: A critical review, Progress in Natural Science, 19 (2009) 291-312.

[102] J. Deign, Siemens tests breakthrough thermal storage system for wind, in: Green Tech Media, 2016.

[103] Y. Gogus, Energy Storage Systems - Volume I, EOLSS, 2009.

[104] M. Jokiel, Development and performance analysis of an object oriented model for phase change material thermal storage, SINTEF Energy Research, 2016.

[105] F. Souayfane, F. Fardoun, P.-H. Biwole, Phase change materials (PCM) for cooling applications in buildings: A review, Energy and Buildings, 129 (2016) 396-431.

[106] Transport av industriell överskottvärme, Svensk Fjärrvarme (Rapport 2009:34), 2009.

[107] F. Setterwall, W. Wang, V. Martin, Preliminary study on heat storage for transportation in Eskilstuna, Technical report ESSAB-4-2009, Ecostorage Sweden AB, 2009.

[108] A. Krönauer, E. Lävemann, S. Brückner, A. Hauer, Mobile Sorption Heat Storage in Industrial Waste Heat Recovery, Energy Procedia, 73 (2015) 272-280.

[109] F. Lele, A thermochemical heat storage system for households, in, Leuphana Universität Lüneburg, Germany, 2016.

Appendix

A. Available PCMs for medium- to high-temperature

Table A.1: Potential PCMs with melting temperature between 80 and 300 °C as summarized by Agyenim et al. [34] (s: solid, l: liquid).

Material	Melting temperature *(°C)*	Heat of fusion *($kJ \cdot kg^{-1}$)*	Density *($kg \cdot m^{-3}$)*	*Specific heat* *($kJ \cdot (kg \cdot K)^{-1}$)*	Thermal conductivity *($W \cdot (m \cdot K)^{-1}$)*
RT100	99	168	940 (s) 770 (l)	1.8 (s) 2.4 (l)	0.2 (s) 0.2 (l)
Na/K/NO3 (0.5/0.5)	220	100.7	1920	1.35	0.56
ZnCl2/KCl (0.319/0.681)	235	198	2480		0.8
ZnCl2	280	75	2907	0.74	0.5

Table A.2: Potential PCMs with melting temperature between 80 and 250 °C as summarized in [35] (s: solid, l: liquid).

Material	Melting temperature (°C)	Heat of fusion ($kJ \cdot kg^{-1}$)	Density ($kg \cdot m^{-3}$)	*Specific heat* ($kJ \cdot (kg \cdot K)^{-1}$)	Thermal conductivity ($W \cdot (m \cdot K)^{-1}$)	Price ($£ \cdot m^{-3}$) ($£ \cdot kWh^{-1}$)
Organic compounds						
Acetamide	82	260	1160 (s)	2.00 (s) 3.00 (l)	0.40 (s) 0.25 (l)	1318 22.2
Oxalic acid	105	356	1900 (s)	1.62 (s) 2.73 (l)		524 3.9
Erythritol	117	340	1450 (s)	2.25 (s) 2.61 (l)	0.73 (s) 0.33 (l)	1287 13.6
Urea	134	250	1320 (s)	1.80 (s) 2.11 (l)	0.80 (s) 0.60 (l)	189 3.0
Maleic acid	141	385	1590 (s)	1.17 (s) 2.08 (l)		1059 9.0
Adipic acid	152	275	1360 (s)	1.87 (s) 2.72 (l)		584 8.4
Salt hydrates						
Magnesium nitrate hexahydrate	89	140	1640 (s)	2.50 (s) 3.10 (l)	0.65 (s) 0.50 (l)	131 3
Oxalic acid dihydrate	105	264	1653 (s)	2.11 (s) 2.89 (l)	0.90 (s) 0.70 (l)	339 4
Magnesium chloride hexahydrate	117	150	1570 (s)	2.00 (s) 2.40 (l)	0.70 (s) 0.58 (l)	56 1
Eutectic compounds						
Urea/NH_4Cl (85/15)	102	214	1348 (s)	1770 (s) 2090 (l)	760 (s) 580 (l)	174 2.3
Urea/NaCl (90/10)	112	230	1372 (s)	1720 (s) 2020 (l)	820 (s) 600 (l)	180 2.1
$LiNO_3/NaNO_3/KNO3$ (30/18/52)	123	140	2068 (s)	1170 (s) 1440 (l)	790 (s) 530 (l)	979 25
$LiNO_3/KNO_3$ (34/66)	133	150	2018 (s)	1170 (s) 1350 (l)	960 (s) 520 (l)	2167 26
$KNO_3/NaNO_3/NaNO_2$ (53/6/41)	142	110	2006 (s)	1170 (s) 1730 (l)	720 (s) 570 (l)	497 8.3
$LiNO_3$/KCl (58/42)	160	272	2196 (s)	1260 (s) 1350 (l)	1310 (s) 590 (l)	3409 21
HCOONa/HCOOK (45/55)	176	175	1913 (s)	1150 (s) 930 (l)	630 (s) 430 (l)	421 4.6
$LiNO_3/NaNO_3$ (49/51)	194	262	2317 (s)	1350 (s) 1720 (l)	870 (s) 590 (l)	3084 19
$LiNO_3$/NaCl (87/13)	208	369	2350 (s)	1540 (s) 1560 (l)	1350 (s) 630 (l)	5254 22
KNO_3/KOH (80/20)	214	83	1905 (s)	1030 (s) 1350 (l)	880 (s) 540 (l)	611 14
$KNO_3/NaNO_3$ (55/45)	222	110	2028 (s)	1010 (s) 1490 (l)	730 (s) 510 (l)	482 8.0
$NaNO_3$/NaOH (86/14)	250	160	2241 (s)	1190 (s) 1860 (l)	660 (s) 600 (l)	339 3.5

Table A.3: Inorganic substances with melting temperature between 300 °C and 600 °C and with potential as PCM summarized by Liu et al. [29] (s: solid, l: liquid).

Material	Melting temp. *(°C)*	Heat of fusion *(kJ·kg^{-1})*	Density *(kg·m^{-3})*	Specific heat *(kJ·(kg·K)$^{-1}$)*	Thermal conductivity *(W·(m·K)$^{-1}$)*	Thermal expansion coeff. *(K^{-1})*
$NaNO_3$	306 - 310	172 - 200	2257-2260 (s) 1908 at 306°C (l)	0.5-1.1 (s) 1.665 at 306°C (l)	0.5 (s) 0.514 at 306°C (l)	40.10^{-6}
NaOH	318 - 320	159 - 165	1785 – 2100 (s) 2.08 – 2.15 (l)	0.92 (s)		
KNO_3	330 - 335	95 - 267	2109 - 2110 (s) 1.22 (l)	0.5 – 0.953 (s)	0.5 (s) 0.425 at 335°C (l)	200.10^{-6}
KOH	360 - 380	134 - 150	2040 – 2044 (s) 1.47 (l)	0.5 – 1.34 (s)		
$Mg(NO_3)_2$	426					
$Ca(NO_3)_2$	560	145				

Table A.4: Inorganic eutectics with melting temperature between 300 °C and 600 °C and with potential as PCM summarized by Liu et al. [29] (s: solid, l: liquid).

Material	Melting temp. *(°C)*	Heat of fusion *(kJ·kg^{-1})*	Density *(kg·m^{-3})*	Specific heat *(kJ· (kg·K)$^{-1}$)*	Thermal conductivity *(W·(m·K)$^{-1}$)*
LiOH/KOH (40/60)	314	341			
KNO_3/KCl (95.5/4.5)	320	74	2100 (s)	1.21 (s)	0.5 (s)
KNO_3/KCl (96/4)	320	150			
KNO_3/KBr/KCl (80/10/10)	342	140			
NaCl/KCl/LiCl (33/24/43)	346	281			
NaOH/NaCl (80/20)	370	370			
$MgCl_2$/KCl/NaCl (60/20.4/19.6)	380	400	1800 (s)	0.96 (s)	
$Li_2CO_3/K_2CO_3/Na_2CO_3$ (32.1/34.5/33.4)	397	276			
$MgCl_2$/KCl (39/61)	435	351	2110 (s)	0.80 (s) 0.96 (l)	 0.81 (l)
$MgCl_2$/NaCl (52/48)	450	430	2230 (s)	0.92 (s) 1.00 (l)	 0.95 (l)
$MgCl_2$/KCl (64/36)	470	388	2190 (s)	0.84 (s) 0.96 (l)	 0.83 (l)
$MgCl_2$/KCl/$CaCl_2$ (48/25/27)	487	342	2530 (s)	0.80 (s) 0.92 (l)	 0.88 (l)
$CaCl_2$/NaCl (67/33)	500	281	2160 (s)	0.84 (s) 1.00 (l)	 1.02 (l)
NaCl/KCl/$CaCl_2$ (29/5/66)	504	279	2150 (s)	1.17 (s) 1.00 (l)	 1.00 (l)
$BaCl_2$/KCl/NaCl (53/28/19)	542	221	3020 (s)	0.63 (s) 0.80 (l)	 0.86 (l)
$BaCl_2$/KCl/$CaCl_2$ (47/24/29)	551	219	2930 (s)	0.67 (s) 0.84 (l)	 0.95 (l)

Table A.5: Metals and metal alloys with melting temperature between 300 °C and 600 °C and with potential use as PCM summarized by Liu et al. [29] (s: solid, l: liquid).

Material	Melting temp. *(°C)*	Heat of fusion *($kJ \cdot kg^{-1}$)*	Density *($kg \cdot m^{-3}$)*	Specific heat *($kJ \cdot (kg \cdot K)^{-1}$)*	Thermal conductivity *($W \cdot (m \cdot K)^{-1}$)*
Pb	328	23			
Al	660	397			
Cu	1083	193.4	8800-8930 (s)		350 (s)
Mg–Zn (46.3/53.7 wt%)	340	185	4600 (s)		
Zn–Al (96/4 wt%)	381	138	6630 (s)		
Al–Mg–Zn (59/33/6 wt%)	443	310	2380 (s)	1.63 (s) 1.46 (l)	
Mg–Cu–Zn (60/25/15 wt%)	452	254	2800 (s)		
Al-Si-Cu-Mg (64.6/5.2/28/2.2wt%)	507	374	4400 (s)		
Al–Cu–Mg–Zn (54/22/18/6wt%)	520	305	3140 (s)	1.51 (s) 1.13 (l)	
Al–Cu (66.92/33.08 wt%)	548	372	3600 (s)		
Al–Si (87.76/12.24 wt%)	557	498	2540 (s)		
Al–Si–Cu (65/5/30 wt%)	571	422	2730 (s)	1.30 (s) 1.20 (l)	
Al–Si (12/86 wt%)	576	560	2700 (s)	1.038 (s) 1.741 (l)	160 (s)

B. Thermal energy storage: key figures

Table B.1: Key figures from examples of thermal energy storage methods using sensible, latent and thermochemical heat storage.

Thermal energy storage methods	*Volumetric energy density ($kWh \cdot m^{-3}$)*	*Investment costs ($NOK \cdot kWh^{-1}$)*	*Temperature range (°C)*	*Typical heat output*	*Lifetime (years)*	*Typical storage capacity*	*Charging time (h= hours, d=days, w=weeks, m=months)*	*Storage time*	*Dischar-ging time*	*Thermal efficiency (%)*	*TRL level*	*Examples of applications*	*References*
Sensible heat storage													
Small water accumulator/tank	10 - 50	20 - 100	0 - 100	1 - 10 kW	10 - 30	1 - 5000 kWh	h	h	h	90 - 98	9	Short-term hot water storage in buildings, small industrial processes	[48, 86-88]
Large water accumulator/tank	10 - 80	20 - 120	15 - 100	0.01 -10 MW	10 - 30	5 - 900 MWh	d - w	w - m	w	90	9	Large scale thermal energy storage, seasonal storage (low temperature)	[86, 87]
Molten salts / high-temperature oils	30 - 100	5 - 200	100 - 500	10 - 50 MW	10-30	0.1 - 500 MWh	h - d	w	h - d	90 - 97	7 - 9	Concentrated solar power, district heating	[48, 89-94]
Soapstone / stones	40 - 75	1000 - 5000	15 - 80	200 - 500 W	30 - 50	2 - 5 kWh	h	h	h	80 - 90	9	Wood stoves, ancient buildings	[95]
Concrete	10 - 80	8 - 250	(-50) - 450	5 - 50 MW	25 - 50	1 MWh - 5 GWh	h - d	h - d	h - d	80 - 95	8 - 9	Concentrated solar power, district heating	[87, 89-91, 96]
Geothermal - boreholes	10 - 80	10 - 100	15 - 90	0.5 - 10 MW	30 - 50	0.1 - 2000 MWh	h - w	w - m	h - w	70 - 90	8 - 9	Large scale thermal energy storage, seasonal storage	[86-88, 97-100]
Geothermal - aquifer	10 - 40	0.3 - 500	20 - 90	0 - 5 MW	10 - 20	500 kWh	h - d	d - w	h - d	65 - 95	8 - 9	Large scale thermal energy storage	[87, 88, 101]
Geothermal – porous rocks	10 - 80	10 - 120	20 - 90	5 - 50 MW	20 - 50	10 - 50 MWh	d - w	m	w	65 - 75	8 - 9	Large scale thermal energy storage, seasonal storage	[87, 100, 102, 103]

Thermal energy storage methods	*Volumetric energy density ($kWh \cdot m^{-3}$)*	*Investment costs ($NOK \cdot kWh^{-1}$)*	*Temperature range (°C)*	*Typical heat output*	*Lifetime (years)*	*Typical storage capacity*	*Charging time*	*Storage time*	*Dischar-ging time*	*Thermal efficiency (%)*	*TRL level*	*Examples of applications*	*References*
Latent thermal energy storage (PCM)													
Low-temperature energy storage	50 - 150	1 - 500	(-30) - 20	1 - 1500 kW	10 - 20	1 kWh - 10 MWh	h - d	d - w	h - d	75 - 90	6 -9	Refrigerated transport, refrigerated cabinets in supermarkets, air conditioning systems	[7, 13, 86, 104]
PCM integrated in building materials	50 - 150	0.5 - 1000	0 - 25	1 - 25 kW	20 - 40	1 - 100 kWh	h	h	h	75 - 90	7-9	Thermal comfort in buildings, air conditioning systems, passive temperature regulation	[40, 43, 86, 100, 105]
Medium-high temperature energy storage	50 - 200	100 - 1000	20 - 600	0.5 - 1500 kW	10 - 20	0.1 - 10 MWh	h	h	h	75 - 90	6 - 8	Hot water production and storage, industrial processes, wood stoves, solar heat production	[43, 48, 87]
Mobile thermal energy storage	75 - 100	200 - 1000	(-20) - 120	0.5 - 1 MW	10 - 20	3 - 4 MWh	h	h - d	h	75 - 90	5 - 7	Transport of industrial excess heat, district heating	[106, 107]
Thermochemical energy storage													
Absorption, adsorption and other chemical reactions	30 - 300	80 - 1000	(-20) - 1200	1 - 500 kW	10 - 20	8 - 5000 kWh	h	h - w	h	75 - 95	3 - 6	Heat transport, heat storage in industrial processes, concentrated solar power	[86, 100, 108, 109]

Technology for a better society

www.sintef.no